

Polymer Chemistry

Accepted Manuscript



This is an *Accepted Manuscript*, which has been through the Royal Society of Chemistry peer review process and has been accepted for publication.

Accepted Manuscripts are published online shortly after acceptance, before technical editing, formatting and proof reading. Using this free service, authors can make their results available to the community, in citable form, before we publish the edited article. We will replace this *Accepted Manuscript* with the edited and formatted *Advance Article* as soon as it is available.

You can find more information about *Accepted Manuscripts* in the [Information for Authors](#).

Please note that technical editing may introduce minor changes to the text and/or graphics, which may alter content. The journal's standard [Terms & Conditions](#) and the [Ethical guidelines](#) still apply. In no event shall the Royal Society of Chemistry be held responsible for any errors or omissions in this *Accepted Manuscript* or any consequences arising from the use of any information it contains.

Cite this: DOI: 10.1039/c0xx00000x

www.rsc.org/xxxxxx

ARTICLE TYPE

Multifaceted Glycodendrimers With Programmable Bioactivity Through Convergent, Divergent, and Accelerated Approaches Using Polyfunctional Cyclotriphosphazenes

Leïla Abbassi,^a Yoann M. Chabre,^{*a} Kottari Naresh,^a Alexandre A. Arnold,^a Sabine André,^b Johan Josserand,^a Hans-Joachim Gabius,^b and René Roy^{*a}

Received (in XXX, XXX) XthXXXXXXXXXX 20XX, Accepted Xth XXXXXXXXXXXX 20XX

DOI: 10.1039/b000000x

We report the sequential construction of a set of multivalent structures using cyclotriphosphazene (CTP) units, which were extensively used as primary or secondary cores implementing branching. The utilization of classical convergent and divergent approaches, together with accelerated dendritic strategies comprising orthogonal sequences, double-exponential and double-stage methodologies will be documented and discussed. Straightforward generation of non-conventional glycodendritic systems with surfaces rich in selectable headgroups, despite a low number of dendrimer generation, was achieved with the efficient assembly of highly functionalized AB₃ and AB₅ nanosynthons. The versatility of the methodology allowed access to a wide variety of structurally diversified platforms. The synthesis was completed by peripheral functionalization with spaced saccharides. The resulting architectures can be drawn as classical globular topologies, also dumbbell shapes and “onion peel” design, referred to as hypercores, wedged hypermonomers, glycoclusters, and glycodendrimers. The convenient implementation of controlled topological diversification is considered instrumental for providing sensitive and potent tools to delineate rules for structure-activity relationships in carbohydrate-protein (lectin) interactions, with possibility to tailor size, valency, ligand density, and topology. To illustrate the applicability of this approach for construction of biologically active glycoconjugates, competitive surface plasmon resonance studies were performed with a bacterial virulence factor and a human adhesion/growth-regulatory lectin and showed multivalent effects.

Introduction

Dendrimers emerged in the late 1970s as monodisperse and hyperbranched macromolecules, whose topologies are likened to three-dimensional tree-like fractal *Lichtenberg* patterns.¹ Their fascinating architecture has since been associated to unique mechanical, biophysical and biochemical properties, largely governed by an extraordinarily high density of active surface functionalities.² Historically, functional groups were first introduced at the periphery of homogeneous and inert dendritic matrices by classical convergent³ and divergent⁴ approaches, often leading to product mixtures. As an additional conceptual drawback, the desired stepwise dendritic growth from a central core required tedious repetitive synthetic steps, at that time involving deprotection/activation sequences that result in rather slow

enhancement in the number of added groups at branch ends in each generation. Gradually, the development of advanced synthetic approaches based on accelerated procedures⁵ and orthogonal sequences^{5a,6} gave rise to sophisticated dendritic architectures of enhanced structural diversity with programmable properties. As a result, while maintaining strict control over the final structures, more complex multifunctional dendrimers have recently been described with compositional diversity including 1) different nature and spatial geometries of terminal functions,^{5a,7} 2) a scaffold allowing orthogonal post-modification⁸ or integrating bioactive moieties,⁹ in contrast to the previously added inert structural elements, 3) different branched building blocks at each generation, as reported in “layer-block”¹⁰ or “onion peel” dendrimers.¹¹ As a result, straightforward access to innovative dendritic materials nowadays drives their ongoing integration into

cutting-edge research fields ranging from nanoengineering to medicine.¹² Owing to their potential to mimic natural glycoconjugates and even membrane surfaces, in terms of topology,¹³ glycodendrimers are considered as valuable tools in the quest to crack the sugar code.¹⁴ Following the pioneering investigations by Yariv *et al.* in the early 1960s,¹⁵ synthetic macromolecular and monodisperse systems, for example glycoclusters¹⁶ and glycodendrimers,¹⁷ also coined as artificial glycoconjugates, have been developed as synthetic tools. Notably, the use of suited multivalent structures, combining selected scaffolds and glycomimetic design, can improve our understanding of recognition mechanisms between the protein interpreters of the glycode, namely the lectins,¹⁸ and their cognate epitopes, in terms of selectivity and specificity. Consequently, studying interactions attributed to the well-documented “glycoside cluster effect”,¹⁹ promises to provide important mechanistic insights into this aspect of biological information transfer, underlying bacterial/viral adhesion and infection,^{17a,b} tumor cell adhesion and aggregation,²⁰ and application of vaccines.²¹ Combining controlled hydrophilic/hydrophobic and rigidity/flexibility balances, associated with adequate density and spatial presentation of epitopes, appear to be key factors for optimizing interactions.²² In this report, we elaborate dendrimer generation from a distinct core system. Starting from the beginning of the 1990s,²³ the potential of phosphorus-based dendrimers as scaffolds with remarkable biodegradable and biocompatible properties is being realized.²⁴ Steps toward applications as drug or gene carriers, anti-HIV agents or fluorescent imaging agents, to name a few, have already been taken.²⁵ However, experience with glycosylated derivatives, particularly cyclotriphosphazene (CTP)-centered glycodendrimers, is still rather limited. To the best of our knowledge, only six studies described their production. Besides purely synthetic reports on the first glycoclusters described in 1983²⁶ and more recently for xyloside derivatives,²⁷ anti-inflammatory²⁸ and anti-adhesin properties^{11a,29} have then been described.

Based on these encouraging observations, we report here, by adapting the large panel of dendritic approaches encompassing well-known convergent, divergent and accelerated approaches, synthesis and testing of functionalized CTP derivatives. A family of original glycodendrimers containing up to 90 glycotopes in a variety in topologies and core frames were prepared and properly characterized. This study complements and extends earlier investigations proposed by Majoral *et al.*, who nicely demonstrated the versatility of multivalent

phosphorus-based dendronized moieties to access complex surface-block, layer-block, and segment-block dendrimers *via* divergent strategies.³⁰ The main advantage of the developed flexible approach is the efficient conjugation of biologically active moieties, *i.e.* spaced lactosides with a controlled number and density, to the periphery. Structural diversity relative to the scaffold itself was also investigated by implementing branching units that confer to each conjugate a distinct size and shape associated with a unique spatial and three-dimensional distribution of epitopes. NMR (1D, 2D, diffusion), mass spectrometry and gel permeation chromatography (GPC) measurements afforded valuable insights to prove assumptions on their required uniformity.

The main goal of the study was to validate the concept that the extensive use of one particular branching unit in all synthetic facets of dendritic construction could generate a series of glycosylated architectures with a complex but programmable structural heterogeneity. In order to document bioactivity of the sugar headgroups and the structural types of design competitive surface plasmon resonance (SPR) assays were used with two different lectins, *i.e.* LecA from *Pseudomonas aeruginosa* and a naturally processed form of a human lectin (trGal-3). Both lectins were chosen due to their physiological relevance as virulence factor and regulator of cell adhesion and growth, respectively.

Results and discussion

Synthesis:

The synthetic strategy was essentially based on the construction of a series of symmetrical and asymmetrical propargylated CTP-based synthons to ensure dendritic growth. Efforts were first directed towards confirming the specific alternated *up and down* geometry of hexapropargylated derivative **1**,³¹ as recently determined with congeners in both solid state and solution (Figure 1).³²

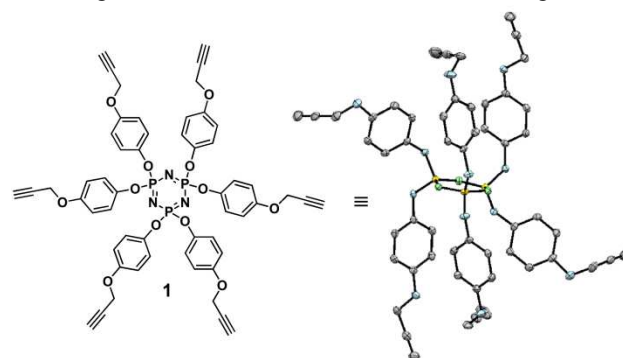
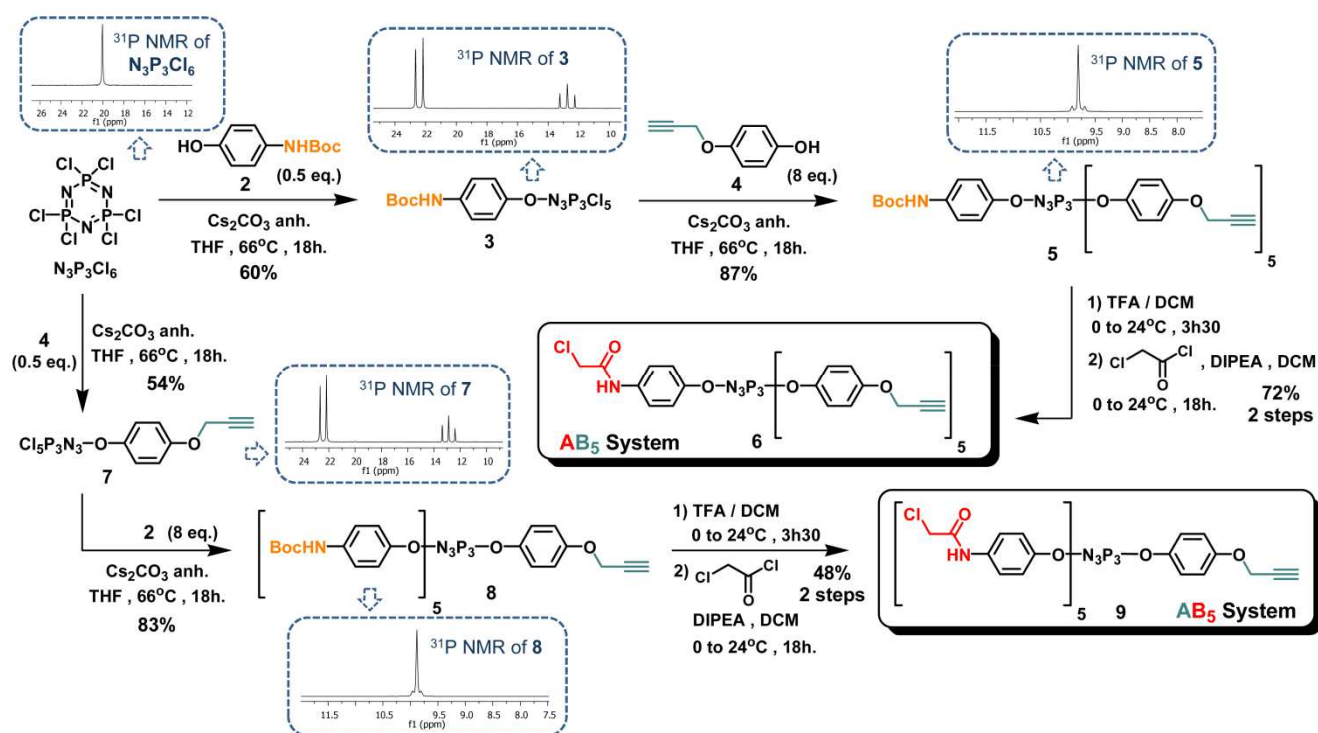


Figure 1. Structure and ORTEP representation at 50% ellipsoid probability of hexapropargylated cyclotriphosphazene **1**. Hydrogen atoms were omitted for clarity.

Recrystallization in a mixture of Et₂O/EtOH/hexanes and resolution of the single-crystal structure by X-ray diffraction analysis led to the expected double tripod pattern with three branches located above the central ring and the other three below (See SI for X-ray data and recrystallization protocol). The characteristic nearly planar cyclotriphosphazene ring with a slight twisted-boat conformation was also observed under these conditions. We next turned our attention towards the synthesis of functionalized AB₅-type building blocks from commercially available hexachlorocyclotriphosphazene (N₃P₃Cl₆). In this context, a desymmetrization process occurred efficiently in our hands through a “1+5” sequence, as recently described.³³ This strategy was based

on the preliminary single displacement of chlorine by a *para*-substituted phenol. The reaction was followed by the five-fold introduction of distinct phenolic derivatives to facilitate further functionalization. The synthesis started from the mono-incorporation of *N*Boc-protected *p*-aminophenol **2**³⁴ on N₃P₃Cl₆, under basic conditions with optimized stoichiometries (core/2/base: 2/1/5 eq. with core freshly recrystallized from hexanes) to furnish the desired precursor **3** in 60% yield (Scheme 1). As expected, this transformation leading to monosubstituted **3** can be monitored by ³¹P NMR spectroscopy that detects the presence of characteristic doublet and triplet signals at 22.4 and 12.9 ppm, respectively (²*J*(P,P) = 59 Hz).³³



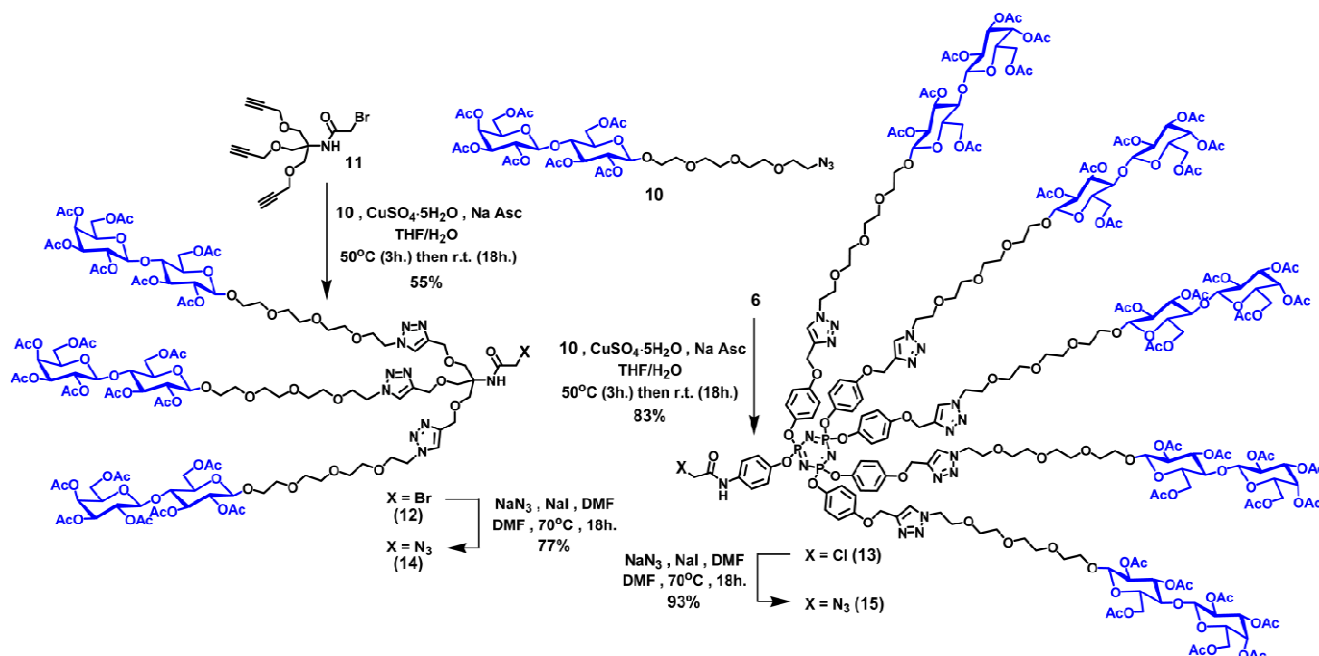
Five units of monopropargylated hydroquinone **4**³⁵ were then introduced with an 87% yield under similar conditions, except for the use of a large excess of phenol **4** and Cs₂CO₃. Once again, multinuclear NMR spectroscopy confirmed the structure of the protected AB₅ building block **5**. Notably, ¹H NMR-spectroscopical monitoring indicated agreement for relative integrations of the five propargylic protons (δ 4.65 and δ 2.52 ppm) compared to the one of the three methyl of the Boc protecting group (δ 2.52 ppm). Furthermore, ³¹P NMR also illustrated completion of the reaction with a symmetrical triplet signal at δ 9.8 ppm. Classical TFA-mediated deprotection, followed by amidation in the presence of an excess of DIPEA and chloroacetyl chloride afforded synthon **6**. It

will represent a key-building block for the synthesis of complex phosphazene-based dendritic architectures. The inverted sequence was also investigated in parallel to obtain synthon **9**. Mono-introduction of phenol derivative **4** was performed with a 54% yield, followed by complete replacement of the remaining five chlorine atoms with **2**. Removal of the five *N*Boc-protecting groups in **8** occurred in the presence of TFA in DCM to obtain the corresponding salt. Final functionalization with chloroacetyl chloride under basic conditions furnished the desired inverted AB₅ system **9** in a 48% yield over two steps.

Glycosylation was achieved with the azide of spacers lactoside **10**³⁶ used as a monomer or presented in a

multivalent display to enable multiplication of the glycotope. Such wedge-like structures were easily synthesized from 1→3³⁷ and 1→5 branching motifs, *i.e.* the known polypropargylated AB₃ TRIS-based derivative **11**^{37b} and AB₅ phosphazene-centered compound **6**, respectively (Scheme 2). In this context, standard *CuAAC*³⁸ conditions were applied for the three-fold grafting of **10** to obtain halogenated dendron **12**. A modified protocol

involving a stoichiometric use of Cu^{II} reagent was necessary to properly access the AB₅ glycosylated congener **13**. Introduction of azido focal function was efficiently performed on both precursors **12** and **13** in the presence of NaN₃ and NaI in DMF to furnish dendrons **14** and **15**, respectively, with good yields.



Scheme 2. Functionalized azido-terminated spaced (tetraethylene glycol-based) β -lactosides (**10**) or corresponding dendronized derivatives (**14** and **15**) used to elaborate complex phosphazene architectures.

In both cases, NMR spectroscopy confirmed the completion of the reactions by revealing disappearance of characteristic signals of propargylic functions in the course of multi-click reactions. Interestingly, ³¹P NMR spectra of glycosylated dendrons **13** and **15** indicated a multiplet ranging from δ 9.4 to 10.2 ppm. This phenomenon, in accordance with observations made by Majoral *et al.*,^{33a} is due to a slightly different distribution of lactoside-terminated branches around the phosphazene core to optimize space occupation, provoking slight modifications of angles around the phosphorous atoms. In addition, the introduction of the azido function in the last step of the sequence was also monitored by FT-IR spectroscopy based on the presence of a band at 2100 cm⁻¹ (See SI).

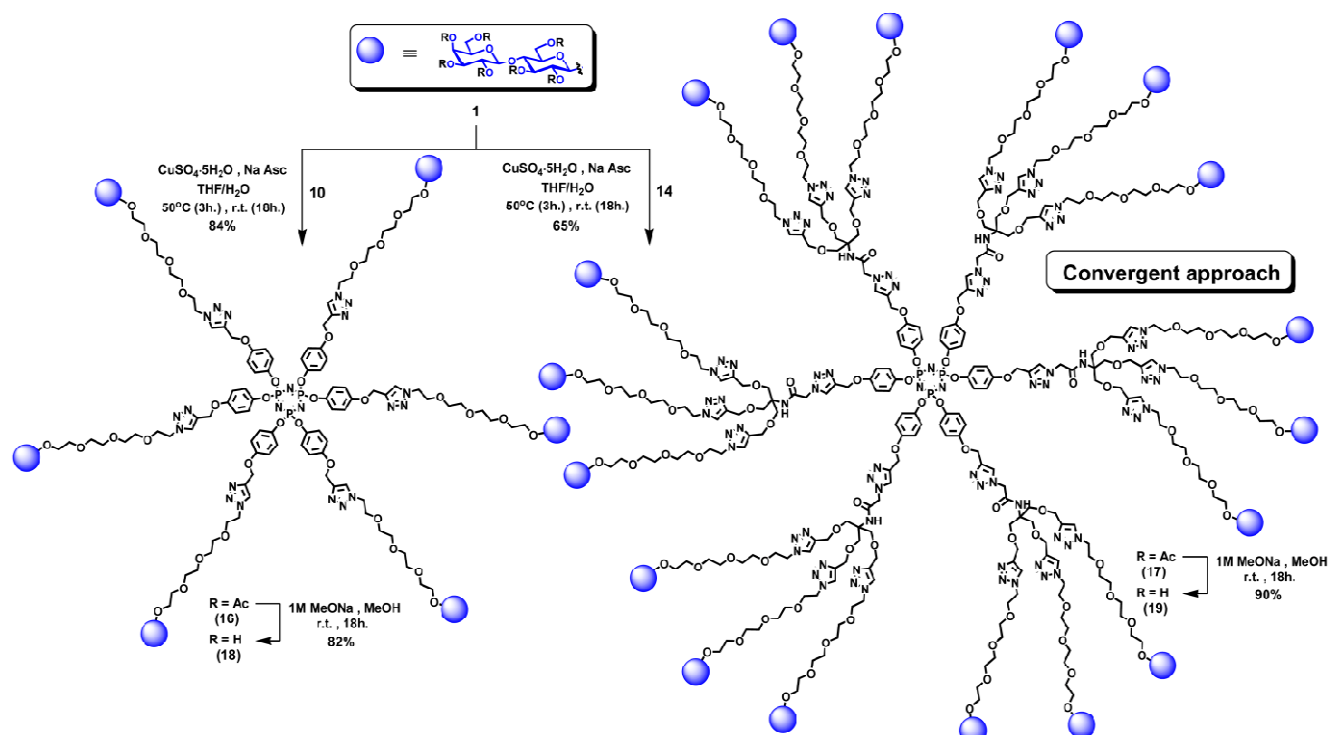
The first members of the CTP-based family with lactosylation were constructed around **1**, on which azides

10 and **14** were incorporated. Bioconjugation was performed in *CuAAC* conditions to provide hexavalent cluster **16** from **10** in an 84% yield. Similar conditions involving dendronized **14** furnished the octadecavalent congener **17** *via* a convergent approach and with a comparable efficiency. The application of a standard Zemplén protocol gave compounds **18** and **19**, from **16** and **17**, respectively (Scheme 3). The ¹H NMR spectra clearly illustrated completion of the multiple click process, notably for **17**, with the entire disappearance of signals belonging to the precursor's propargyl functions at δ 4.65 and 2.64ppm. In addition, all the relative integrations of each triazole protons presented in the external section were in perfect agreement with those of the newly formed internal region (18 vs 6, respectively).

Cite this: DOI: 10.1039/c0xx00000x

www.rsc.org/xxxxxx

ARTICLE TYPE



Scheme 3. Synthesis of hexa- (**18**) and octadeca- (**19**) lactosylated derivatives around CTP core.

Pentavalent hypermonomer **15** was then extensively used for diversified strategies that covered the large spectrum of accelerated dendritic synthesis. Initially, deca-
 5 valent dumbbell-shape lactosylated compound **21** was synthesized using dipropargylated tetraethylene glycol **20**³⁹ as a suitable complementary partner for the double click reaction. De-*O*-acetylation using 1M MeONa in MeOH
 10 quantitatively generated **22**. Orthogonal desymmetrization was also considered with the coupling of **9** and **15** to straightforwardly generate the heteromultifunctional precursor of Janus system **23** in good yield, containing five
 35 reactive chloro *N*-acetyl peripheral appendages (Scheme

4). Due to the non-equivalent nature of all five substituents around both phosphazene cores, **23** gave a ¹H NMR spectrum with particular differences in comparison to that of precursor **15** (Figure 2). Notably, the appearance of two signals at δ 8.96 and δ 8.60 ppm originating from both sets of peripheral amides (integrations of 2 and 3, respectively) was observed, together with the signal of the proton of the newly formed internal triazole group at δ 8.05 ppm. Furthermore, signals of new methylene linkages showed up clearly at δ 5.46 and \sim δ 4.20 ppm with expected relative integrations, corresponding to internal $-\text{N}_{\text{triazole}}\text{CH}_2\text{CONH}-$ and peripheral $-\text{NHCOCH}_2\text{Cl}-$.

Cite this: DOI: 10.1039/c0xx00000x

www.rsc.org/xxxxxxx

ARTICLE TYPE

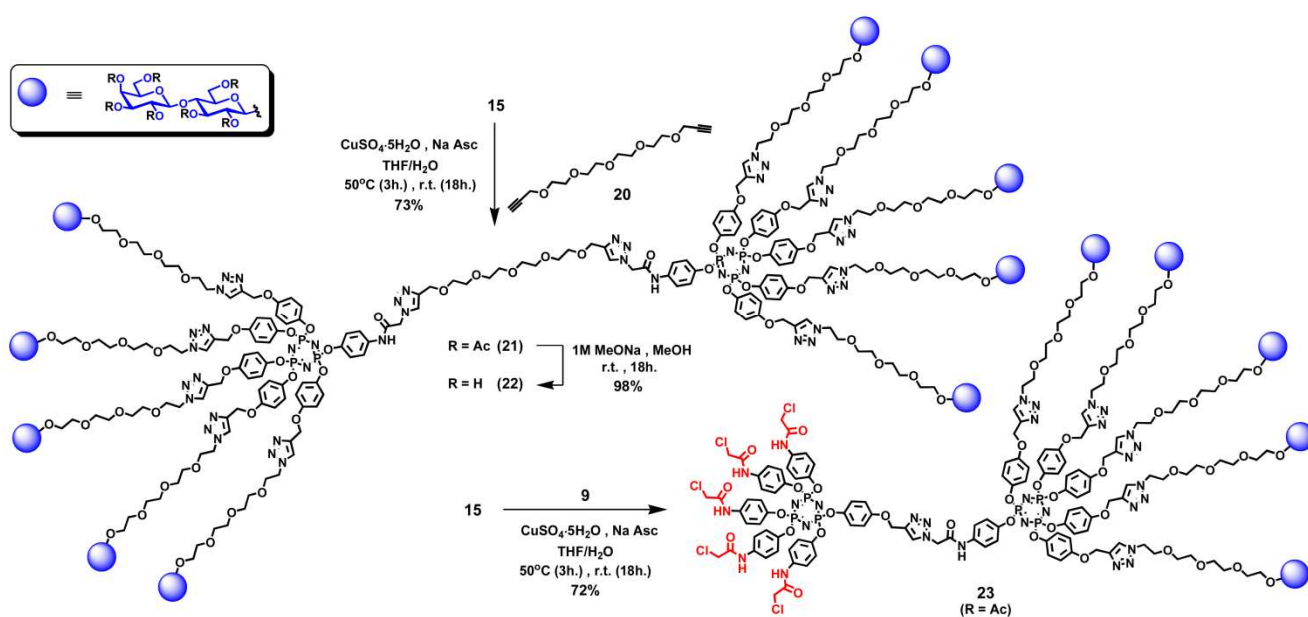
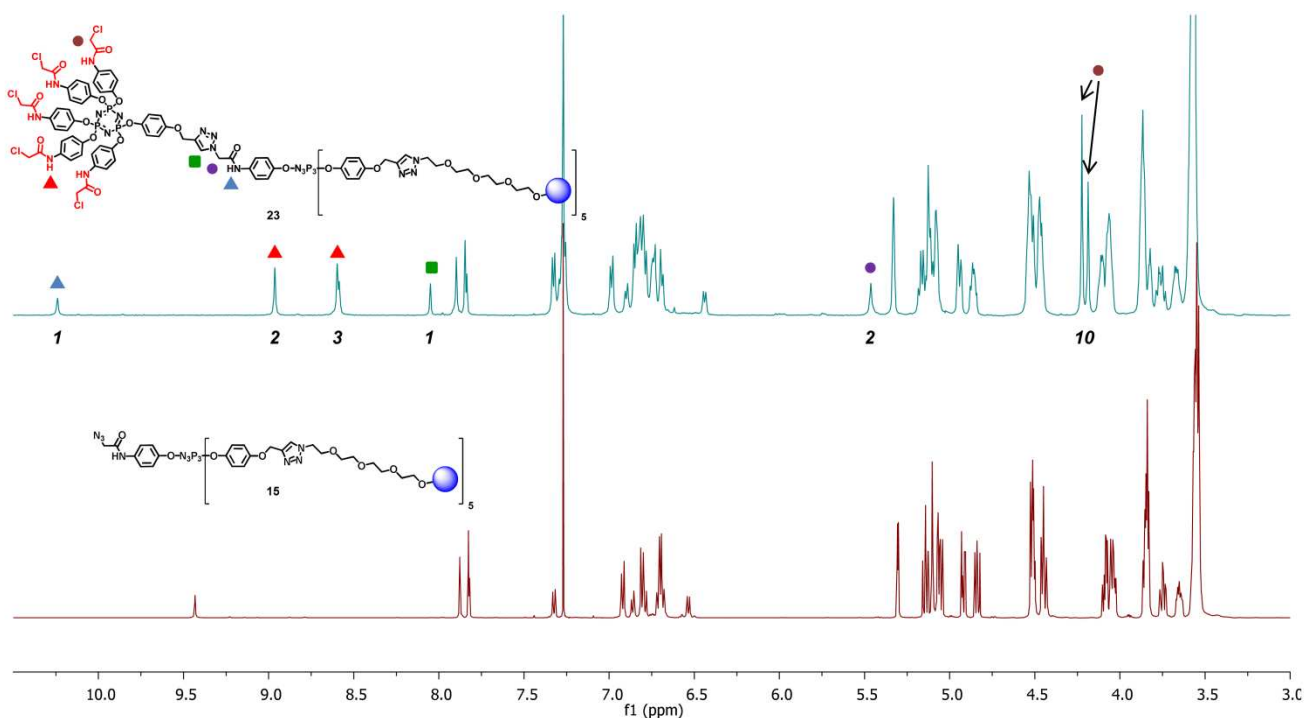
Scheme 4. Synthesis of dumbbell-shape decavalent derivative (**22**) and the heterofunctionalized form **23**.

Figure 2. Comparison of ^1H NMR spectra (CDCl_3 , 600 MHz) of **15** and **23** with the appearance of characteristic signals for asymmetrical compound **23** (top). Observed proton integrations are indicated in italics below each signal of **23**.

Cite this: DOI: 10.1039/c0xx00000x

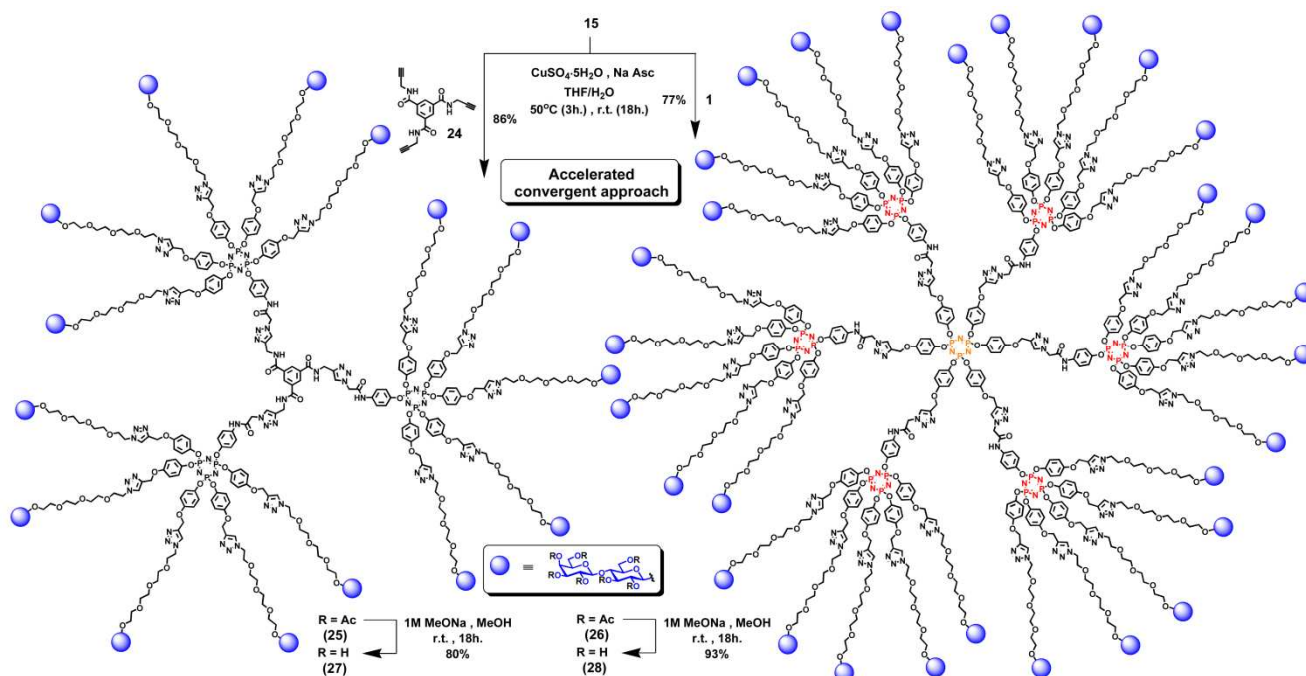
www.rsc.org/xxxxxx

ARTICLE TYPE

Although beyond the scope of this work, we can envision a subsequent transformation of compound **23** based on our recent investigations on orthogonal transformations of *N*-chloroacetylated derivatives with high functional group tolerance strategies.⁴⁰ For instance, multiple *CuAAC* couplings subsequent to the mild introduction of azido functions on **23** or multiple S_N2 reactions with thiol-terminated partners would represent methods of choice to integrate relevant entities, *e.g.* suited glycans, other targeting moieties or drugs.

In order to explore the flexibility of our global synthetic approach and to enhance the density of termini using a limited number of steps, key-dendron **15** was also coupled to different complementary polypropargylated cores through accelerated convergent approaches. The first known trivalent template **24**⁴¹ was subjected to classical *CuAAC* conditions in the presence of **15** to produce pentadecaivalent system **25** in an excellent yield of 86% (Scheme 5). Similar treatment with **1** allowed for the efficient and rapid synthesis of the first G(1)-glycodendrimer scaffolded over two different layers of CTP cores, containing twice the number of epitopes. Thus, trivalent lactodendrimer **26** was obtained in 77%

yield, corresponding to an excellent 96% yield per individual click reaction. Despite the apparent congestion generated by the dendron, the predicted *up and down* distribution around cyclotriphosphazene cores together with the flexibility of the branches were assessed to adequately exhibit reactive complementary functions to ensure the reactions in THF/H₂O mixture. Notably, no traces of the propargylic protons' signal from each precursor, *i.e.* at δ 3.14 ppm for **24** (in DMSO-*d*₆) and δ 2.54 ppm for **1**, were detected, thus confirming completion of the multi-click process. Once again, removal of protecting groups under basic conditions led to conjugates **27** and **28** with deprotected β -lactoside, from **25** and **26**, respectively. MALDI-TOF experiments afforded isotopic patterns for trivalent conjugates **26** and **28** with the expected molecular weight signal ($[M+Na]^+$ adducts) at ~32550 and ~23750 Da, respectively. In addition, iterative regular fragmentation patterns were observed in both cases with successive losses of dendronized and monomeric triazole species (Figure 3). Interestingly, these regular losses were also seen for acetylated **26** in ESI⁺ technique (after deconvolution, *see SI*).



Scheme 5. Synthesis of glycodendrimers containing 15 (**27**) and 30 (**28**) peripheral β -lactoside moieties through an accelerated convergent dendritic approach.

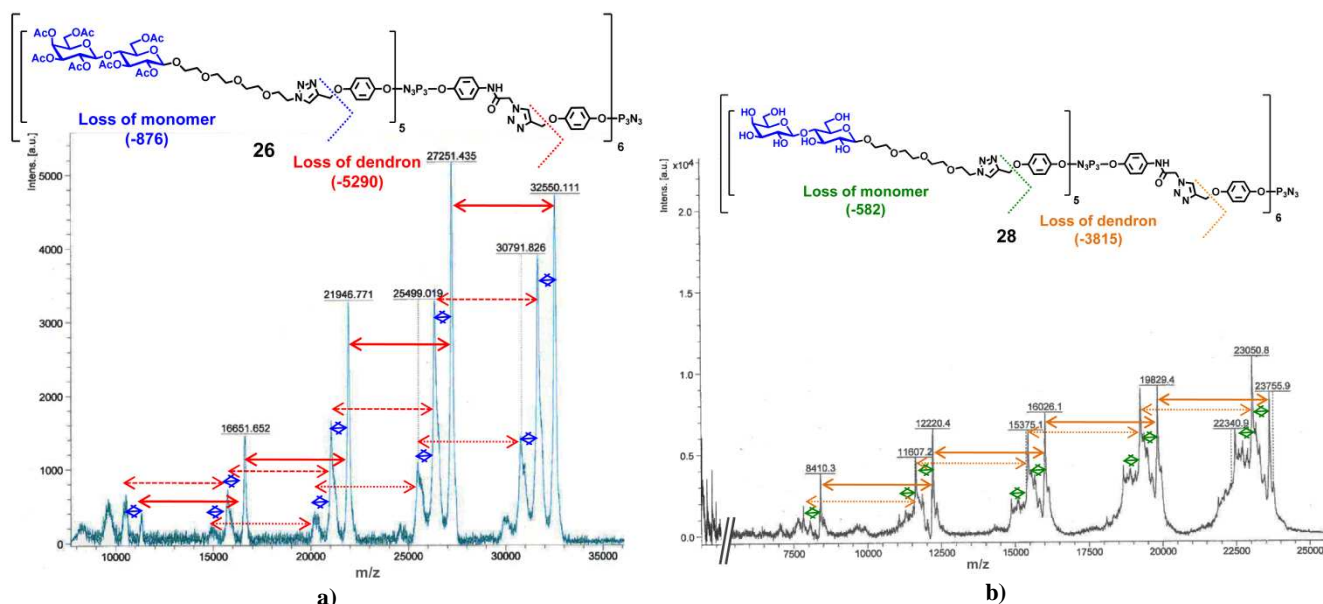


Figure 3. MALDI-TOF spectra of glycodendrimers with a) protected (**26**) and b) deprotected (**28**) β -lactosides (DHB matrix), indicating regular fragmentation patterns with successive loss of monomeric or dendronized species.

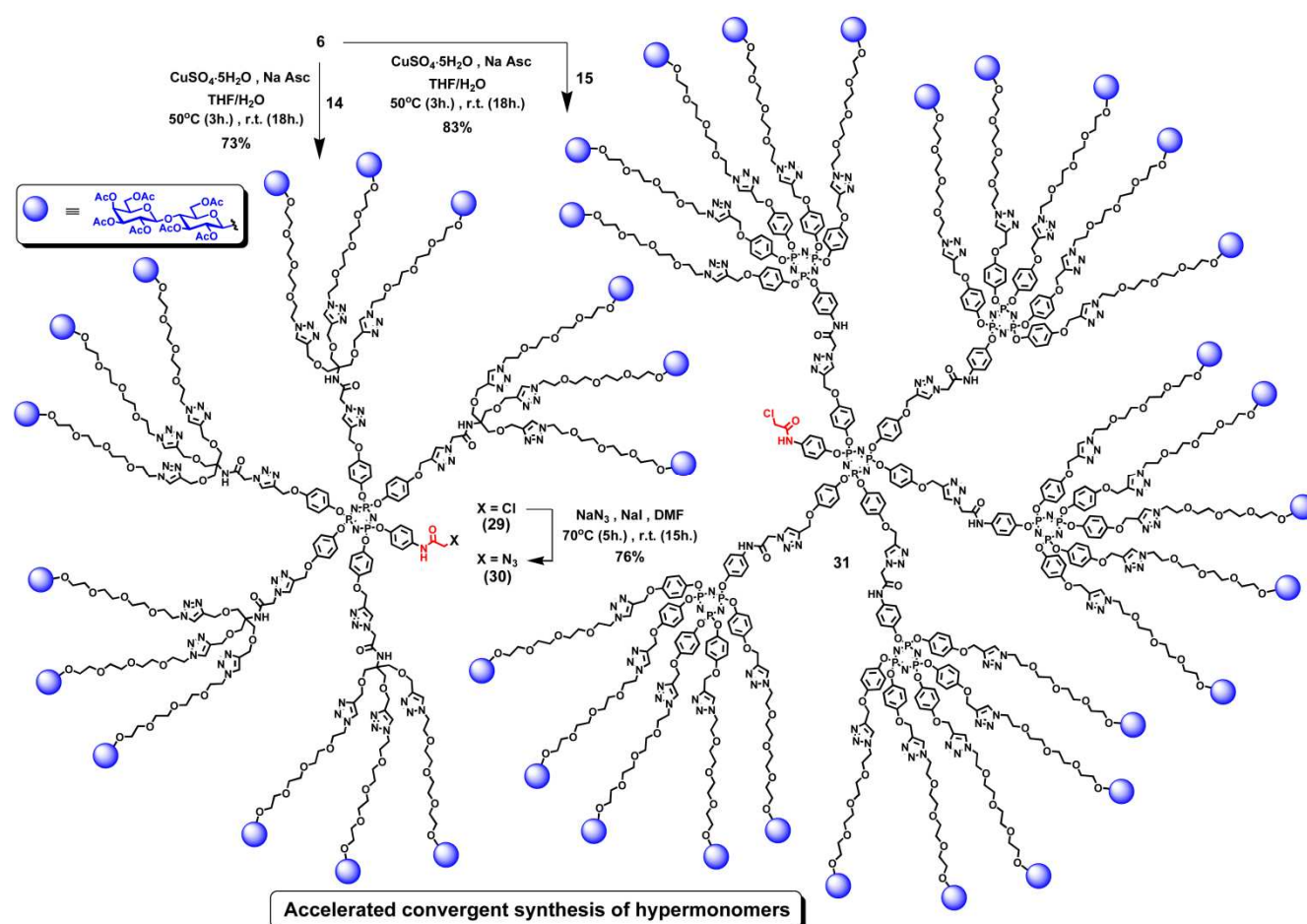
The investigation of accelerated methodologies towards the development of multivalent dendrons carrying sugar units was next extended using pentapropargylated AB_5 secondary core **6**, on which lactosylated dendrons **14** and **15** were successfully grafted (Scheme 6). Once again, Cu^I -catalyzed cycloadditions efficiently gave access to the first AB_{15} system (**29**) in a 73% yield. These encouraging results prompted us to push the limits of this strategy further, proposing the synthesis of G(1) lactosylated dendron **31** containing 25 termini with the application of a double-exponential methodology. An excellent 83% yield was observed for the construction of the AB_{25} wedge *via* the use of a double-exponential methodology from orthogonally functionalized key-synthon **6**. As expected, and as earlier observed for **15** and **17**, the complex multiplet ranging from δ 8.9 to 10.4 ppm was observed in the ^{31}P NMR spectrum, originating from the distinct geometrical environment of each CTP layer that caused slightly different chemical shifts. Also of interest, subsequent derivatizations on the apparently buried focal chloroacetylated function could be easily monitored by 1H and ^{13}C NMR spectroscopy, since distinctive $-COCH_2Cl$

signals are clearly visible for both structures (δ 4.20 and 43.5 ppm, respectively). For instance, chlorine replacement by an azido function furnished **30**, whose 1H and ^{13}C NMR spectra indicated total disappearance of focal halogenated methylene signal. A down-field shifted signal at δ 52.1 ppm corresponding to $-COCH_2N_3$ was observed in the ^{13}C NMR spectrum. It is worth to mention that a novel, highly accelerated convergent approach using AB_{15} hypermonomer **30** and a complementary tripropargylic phloroglucinol-based template has also been tested. Interestingly, NMR spectra unambiguously indicated the three-fold Cu^I -catalyzed coupling of the hypermonomer around the core, with the absence of the characteristic propargylic signals (*See SI* for the synthetic sequence, related structures and discussions). Preliminary spectroscopic data supported the integrity of the desired structure. Unfortunately, in contrast with other structures presented, analytical efforts towards the complete characterization of the resulting structure containing 45 epitopes were unsuccessful.

Cite this: DOI: 10.1039/c0xx00000x

www.rsc.org/xxxxxx

ARTICLE TYPE



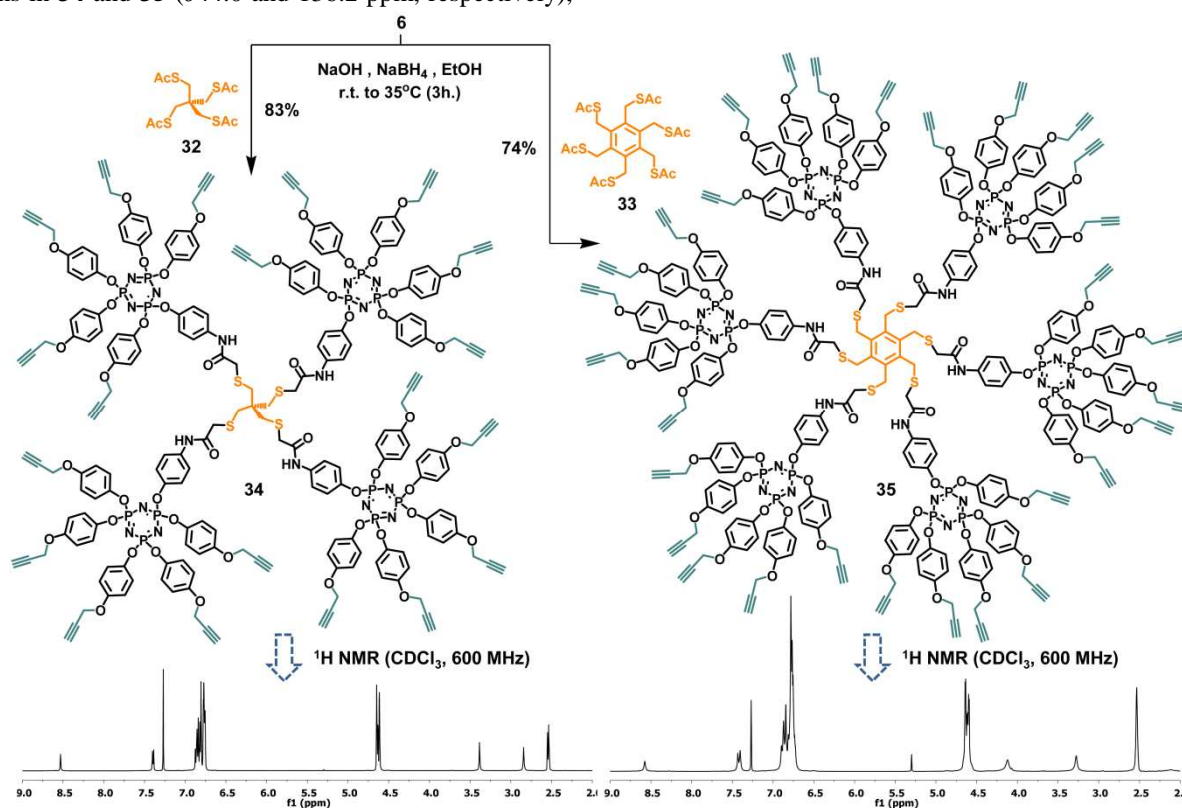
Scheme 6. Synthesis of large lactosylated wedge-like hypermonomers containing 15 (**29-30**) and 25 (**31**) epitopes and one reactive focal function through an accelerated convergent strategy.

The aim to cover all aspects of accelerated dendritic approaches around one type of synthon prompted us to investigate the elaboration of CTP-based “multifunctional cores”. Toward this end, corresponding “hypercores”^{51,5j} were successfully synthesized according to a known strategy based on the use of poly-thioacetylated cores and complementary *N*-chloroacetamide-terminated dendrons.³⁷ In this context, using standard basic and reductive conditions (NaOH/NaBH₄ in EtOH) on **6**, in the presence of known aliphatic (**32**) or aromatic (**33**) cores,^{37b} the formation of highly symmetrical icoso- (**34**) and tricon-
 15 propargylated (**35**) hypercores, respectively, was accomplished (Scheme 7). The reduced number of synthetic steps and the generation of a high density of functions without prerequisite activations constitute notable advantages in the quest for routes to achieve rapid

dendritic growth. Satisfactory yields were obtained for both derivatives, with reduced reaction times (3h). The insolubility of the products in ethanolic media made their purification easy, since excess of soluble reactants was removed by successive EtOH washing. Noteworthy is the fact that attempts involving previously optimized conditions (excess of 1M MeONa in MeOH with similar but simplified systems)⁴⁰ generated desired derivatives but in lower yields and with more tedious purification. Besides
 45 satisfactory mass spectrometry results, especially for compound **34** (high resolution ESI⁺), whose experimental $[M+2Na]^{2+}$ and $[M+3Na]^{3+}$ adducts matched the theoretical patterns (Figure 4), ¹H and ¹³C NMR spectra unequivocally confirmed the completion of the multiple S_N2 reactions in
 50 both cases. The high symmetry led to simple ¹H spectra with the presence of distinct pair of signals corresponding

to the $-CH_2-$ in each inner section (δ 3.39 and 2.84 ppm for **34** and δ 4.12 and 3.28 ppm for **35**), with expected relative integrations (Scheme 7). In addition, the presence of a specific and unique signal in ^{13}C NMR spectra, corresponding to the central quaternary and aromatic carbons in **34** and **35** (δ 44.0 and 136.2 ppm, respectively),

further emphasized the monodispersity of the structures. In accordance with our previous investigations,^{37b} these observations unambiguously allowed to exclude an unwanted polymerization process through oxidation of thiols generated *in situ*.



Scheme 7. Synthesis of hypercores **34** and **35** containing 20 and 30 peripheral propargylated functions, respectively, together with 1H NMR spectra ($CDCl_3$, 600 MHz) indicating completion of S_N2 reactions.

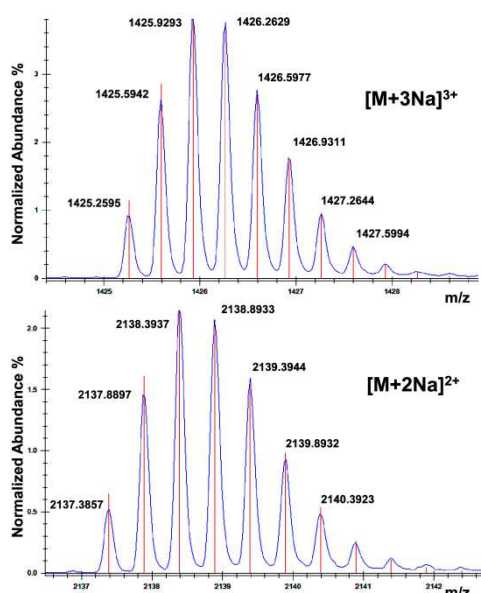


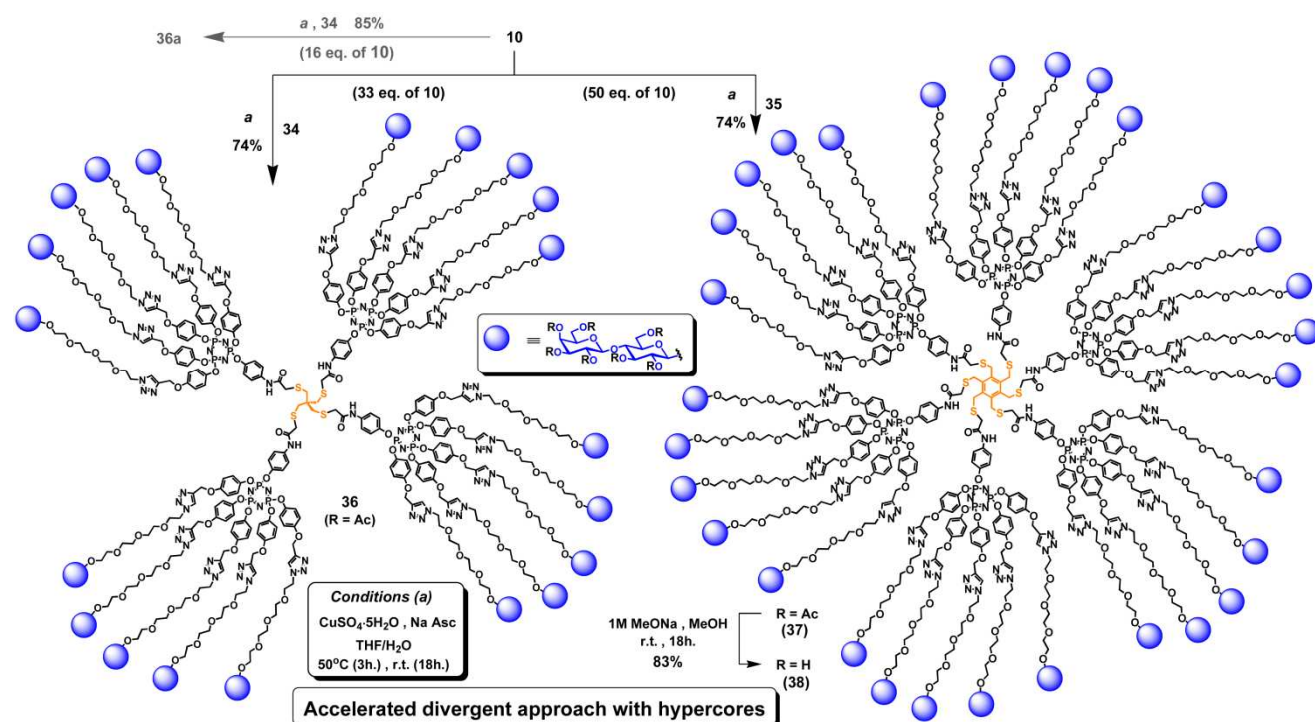
Figure 4. Zoomed section of isotopic distributions of $[M+3Na]^{3+}$ (top) and $[M+2Na]^{2+}$ (bottom) adducts for **34** (ESI⁺-HRMS). Experimental signals are in blue and theoretical patterns are in red.

The introduction of epitopes around these hypercores first proceeded through the application of a divergent methodology. In that context, *CuAAC*-mediated conjugation using monomeric azido lactoside **10** in excess (1.7 eq./propargylic function) efficiently afforded macromolecules **36** and **37** with 20 and 30 termini, respectively (Scheme 8). Similar yields of 74% were observed, corresponding to an excellent $\geq 98\%$ yield per individual reaction. Characterization of **36** by 1H NMR particularly gave predictable signals with expected relative integrations, comparing distinct H_{4gal} (δ 5.30 ppm, 20H), triazole (δ 7.85 ppm, 20H), and internal C_qCH_2S- (δ 2.80 ppm, 8H) protons. In addition, the absence of propargylic signals, both in 1H and ^{13}C NMR spectra further confirmed the completion of the multiple processes.

Cite this: DOI: 10.1039/c0xx00000x

www.rsc.org/xxxxxx

ARTICLE TYPE



Scheme 8. Synthesis of icosadendritic (**36**) and trivalent (**37** and **38**) glycodendritic structures from hypercores **34** and **35** through an accelerated divergent approach. Conditions to create a controlled number of structural defects from **34** are mentioned in grey.

Interestingly, the use of sub-stoichiometric quantities of lactoside **10** (16.0 eq. for 20 propargylic functions) generated a mixture of multivalent species with structural defects (**36a**), harboring unreacted internal propargylic functions whose presence (~4) can be clearly detected by NMR spectroscopy (Figure 5). For this special case, the expected remaining alkyne signals at δ 2.53 and ~4.65 ppm in the structures were seen. Together with characteristic signals at ~ δ 78.0 and 76.0 ppm, an even more intense signal at δ 56.1 corresponding to peripheral $-\text{OCH}_2\text{C}\equiv\text{CH}$ in ^{13}C NMR spectroscopy was clearly detectable. 2D COSY and HSQC experiments reinforced all the expected correlations (See SI). From a synthetic perspective, monitoring of introduction of structural defects aimed at confirming the integrity and monodispersity of flawless macromolecules elaborated *via* optimized protocols with an excess of lactosides, *i.e.* **36**, **37** and resulting deprotected **38**. Eventually, access to straightforward post-functionalization can be considered with the subsequent grafting of complementary azido-probes, guiding moieties such as carbohydrates or drugs to remaining propargylated functions present in **36a**.

The same hypercores **34** and **35** were subsequently used for the synthesis of hypervalent glycoconjugates decorated with 60 and 90 epitopes from the anchorage of trivalent dendron **14** with optimized stoichiometries (1.750 eq./propargyl). This approach differed from the one previously described by the combined use of hypercores and lactosylated wedges, thus representing an accelerated convergent double-stage approach. The presence of TRIS-based dendrons generated more complex structures resulting in the placement of concentric and distinct layers based on different functional groups and building blocks around a central core moiety. In this respect, “onion peel” glycodendrimers have been synthesized around an aliphatic or aromatic core, surrounded successively by AB_5 -phosphazene and external AB_3 -TRIS-based layers. A rapid dendritic growth from 2 steps-20 \times 3 or -30 \times 3 sequences generated densely packed, lactose-bearing compounds **39** and **40** with yields similar to those observed for the latter inside-out approach, *i.e.* with excellent \geq 98% yields per individual triazole formation (Scheme 9).

Cite this: DOI: 10.1039/c0xx00000x

www.rsc.org/xxxxxx

ARTICLE TYPE

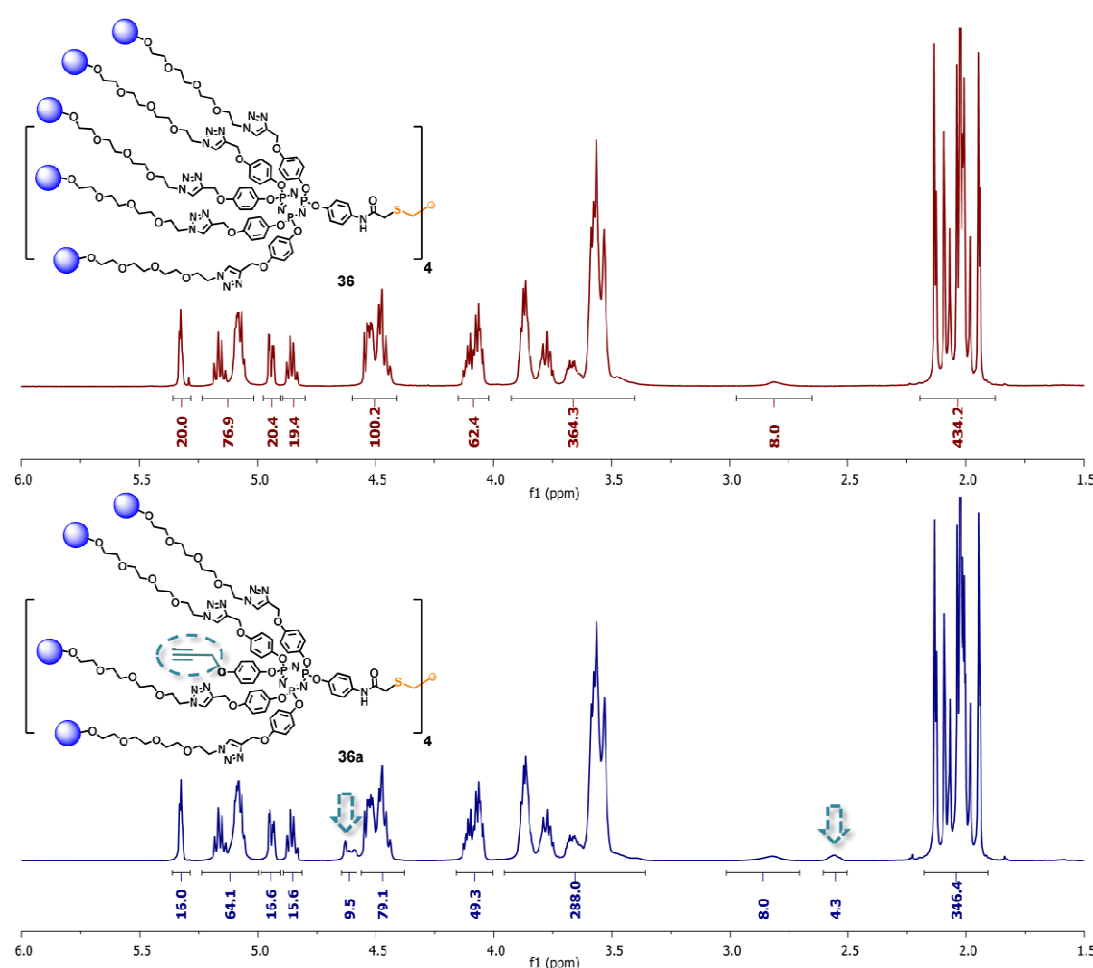


Figure 5. ^1H NMR (600 MHz, CDCl_3) comparison between perfect monodisperse icosavalent macromolecule **36** and mixture of defective congeners **36a** presenting an average of 16 peripheral termini and 4 buried propargylic functions ($\delta 2.53$ for $\text{C}\equiv\text{CH}$ and ~ 4.65 ppm for $\text{OCH}_2\text{C}\equiv\text{CH}$ in this particular case).

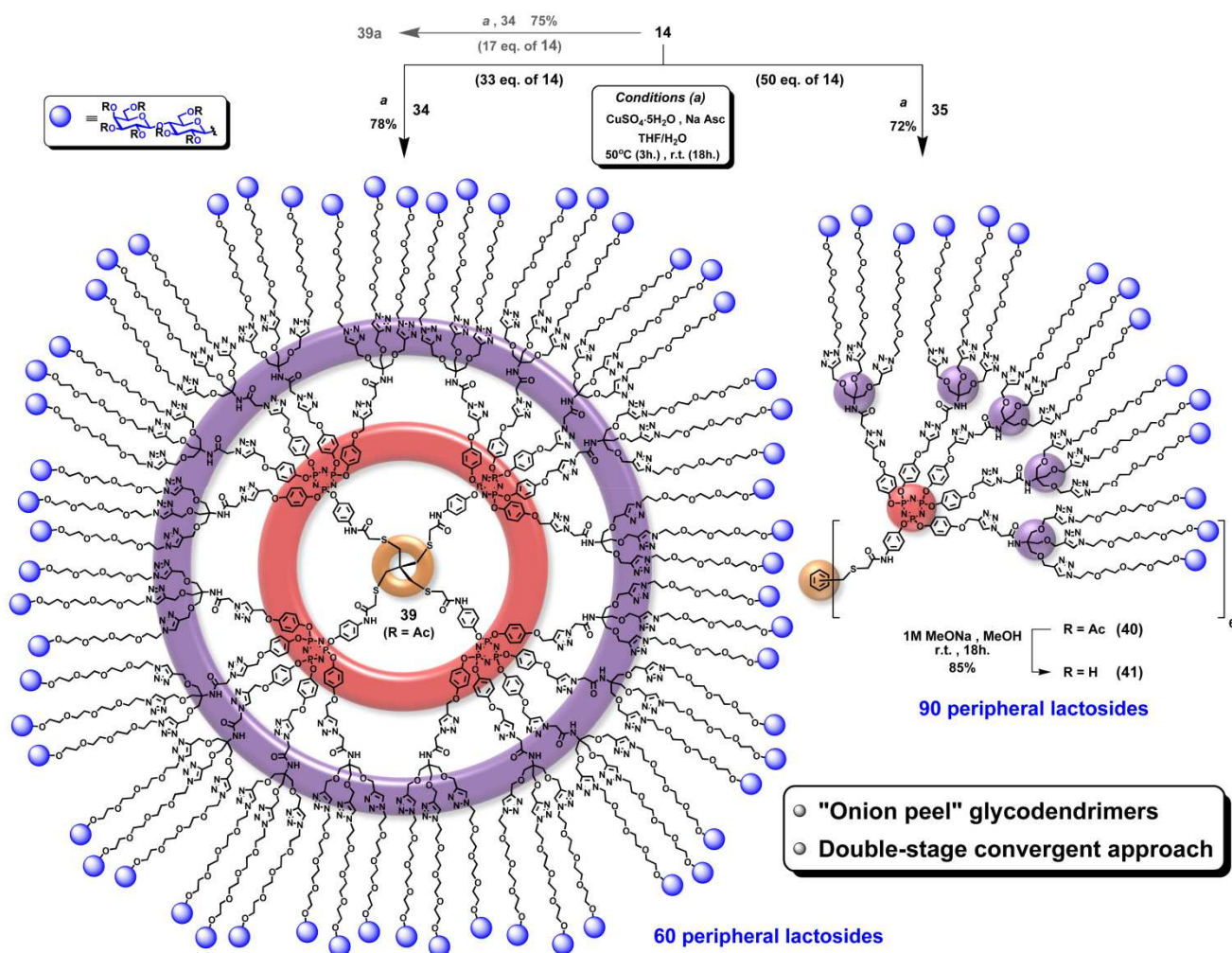
The present methodology thus represents an elegant alternative to the divergent sequences described earlier by our group for the elaboration of “onion peel” structures.^{11a} A similar protocol ensuring presence of structural defects was further applied to confirm that a limited number of remaining propargylated functions in a more complex structure can also be monitored by NMR. To this end, a sub-stoichiometric amount of **14** (17 eq. for 20 propargylic functions) and core **34** were engaged under classical click chemistry conditions. As expected, the entirety of the dendron was consumed at the end of the reaction, as indicated by TLC. More notably, ^1H NMR (600 MHz) and DOSY spectra of **39a** revealed the ~ 3 signals from remaining buried propargylic functions with characteristic

chemical shifts ($\delta 2.60$ for $\text{C}\equiv\text{CH}$ and ~ 4.75 ppm for $\text{OCH}_2\text{C}\equiv\text{CH}$ in this particular case), although at the limits of detection. Spectra of flawless structure **39** compared well with those of defective **39a**, with the unequivocal absence of the characteristic propargylic signals in ^1H and ^{13}C NMR spectroscopy (notably at $\delta 56.1$ ppm corresponding to $-\text{OCH}_2\text{C}\equiv\text{CH}$, 3 days of acquisition, 145000 scans at 150 MHz, *See SI*). Finally, de-*O*-acetylation of **40** completely took place to afford nonacontavalent derivative **41**. Note that this glycodendrimer with 630 peripheral OH functions was efficiently built in a reduced number of synthetic steps and represents on its own a hyperfunctionalized platform for further modification or direct applications.

Cite this: DOI: 10.1039/c0xx00000x

www.rsc.org/xxxxxx

ARTICLE TYPE



Scheme 9. Synthesis of hexaconta- (**39**) and nonacontavalent (**40** and **41**) "onion peel" glycodendritic structures from hypercores **34** and **35**, via a double-stage convergent approach. Conditions to create a controlled number of structural defects from **34** and sub-stoichiometric amount of dendron **14** are also indicated.

5 Besides NMR-spectroscopical analysis, the characterization of the novel set of dendritic structures was completed with GPC and mass spectrometry measurements (Table 1). Remarkably, in all cases except for **40**, GPC data indicated very low polydispersity indexes for acetylated compounds (PDIs (M_w/M_n) ≤ 1.08) with single narrow Gaussian patterns and M_w values that compare well with the ones obtained with MS experiments. Complementary biophysical investigations were also conducted to evaluate the size progression and the three-dimensional shapes of all the multivalent derivatives. In this context, diffusion NMR spectroscopy has recently become a method of choice to obtain information on the

hydrodynamic behavior of macromolecular species by measuring their diffusion coefficients in a given solvent.^{22b,41,42} The size of the glycodendrimers containing the acetylated and the deprotected derivatives, and more particularly their solvodynamic radii, was estimated by pulsed-field-gradient stimulated echo (PFGE-STE) NMR experiments using bipolar pulse pairs-longitudinal-eddy-current delay (BPP-LED) in CDCl₃ and D₂O, respectively, at 25°C.⁴³ Stimulated echoes were used, they avoid signal attenuation due to transverse relaxation, while bipolar gradient pulses reduce gradient artifacts.⁴⁴ To determine the overall diffusion coefficient (D) of each construct, an increasing field gradient strength was applied. D values

were determined by the average of individual values corresponding to the decay of the signal intensity of different protons located at different level in the molecule (Table 2). Interestingly, mono-exponential behavior was observed for specific, distinctive and common protons (*i.e.* at δ 5.34 ppm relative to H_{4gal} for acetylated derivatives and at δ 7.90 ppm for $H_{triazole}$ of hydroxylated compounds), which manifested as a linear decay of the logarithm of the signal intensity as a function of the gradient strength

squared (*See SI*). This behavior was consistent with the spherical and unimolecular character of the evaluated glycodendrimers and also observed from other protons located either in internal regions, including the dendritic core and connecting branches, or in the peripheral saccharidic belt (results not shown). In this context, application of the Stokes-Einstein equation directly yielded the corresponding solvodynamic diameters ($d_s = 2 \times r_s$), using viscosities determined for pure deuterated solvents.

Table 1 GPC and mass spectrometry data for peracetylated dendritic derivatives.

Cpd	GPC ^{a,b,c}			Mass spectrometry ^d		
	M_w	M_n	PDI (M_w/M_n)	Calcd M_w	Found	Technique
15	5462	5367	1.02 ^a	<i>5247.7180</i>	<i>1750.2466 [M+3H]³⁺</i>	ESI ⁺ -HRMS
16	6882	6764	1.02 ^a	<i>6041.0072</i>	<i>1511.5123 [M+4H]⁴⁺</i>	ESI ⁺ -HRMS
17	21740	21350	1.02 ^b	18008.6	18008.5 [M+H] ⁺	ESI ⁺ (deconv.)
21	10410	10180	1.02 ^b	10772.8	10772.5 [M+H] ⁺	ESI ⁺ (deconv.)
23	7981	7889	1.01 ^a	<i>6449.7757</i>	<i>1636.6848 [M+4Na]⁴⁺</i>	ESI ⁺ -HRMS
25	18970	18820	1.01 ^a	16074.6	16074.1 [M+H] ⁺	ESI ⁺ (deconv.)
26	35320	34480	1.03 ^b	32523.3	32523.7 [M+H] ⁺	ESI ⁺ (deconv.)
					32550.1	MALDI-TOF
30	16580	15400	1.08 ^a	15221.1	15220.6 [M+H] ⁺	ESI ⁺ (deconv.)
31	26040	25230	1.03 ^b	27309.0	27241.4	MALDI-TOF
34	4625	4540	1.02 ^c	<i>4272.7557</i>	<i>2137.3851 [M+2H]²⁺</i>	ESI ⁺ -HRMS
35	7152	6399	1.12 ^a	6467.7	6468.9	MALDI-TOF
36	25870	24610	1.05 ^b	21031.3	21098.1	MALDI-TOF
37	42710	39580	1.08 ^b	31600.9	31478.0	MALDI-TOF
39	76570	75530	1.01 ^b	60908.9	~ 60000-centered Gaussian	MALDI-TOF

^a GPC was performed using THF as eluent.

^b GPC was performed using (CHCl₃/Et₃N (1%)) as eluent.

^c GPC was performed using CHCl₃ as eluent.

^d Exact mass values are indicated in italics when high-resolution analyses were performed (ESI⁺-HRMS). Low-resolution mass values were obtained using MALDI-TOF (DHB matrix) or ESI⁺ (after deconvolution, [M+H]⁺ adducts) techniques. Mass spectrometry data for fully deprotected compounds (**18**, **19**, **22**, **27**, **28**, **38**, and **41**) and **40** are detailed in SI section.

As expected, *D* values revealed the increase of the solvodynamic diameters as the number of peripheral epitopes was enhanced, under similar solvent conditions. Consistent tendencies were observed throughout the same acetylated or deprotected compounds comprising dendrons and globular clusters and dendrimers with solvodynamic diameters ranging from 2.6 to 10.1 nm. Interestingly, despite distinct dendritic templates, identical values were obtained for pentadecavalent systems **25** and **29** (entries 6 and 2). Coherent results were also obtained when comparing diameters of dendron **31** and that of corresponding “flawless” glycodendrimer **26** (6.8 and 7.5 nm, respectively) (entries 3 and 9). On the contrary,

scaffolding around different dendritic cores generated slight discrepancies in diameter values for acetylated or deprotected trivalent systems (**26** vs **37** and **28** vs **38**, respectively). In addition, related to the series of protected derivatives built around hypercores, *i.e.* **36**, **37**, **39** and **40**, no trends could be established, because the pentaerythritol core alternatively generated either smaller (**39** vs **40**) or bigger (**36** vs **37**) systems compared to the corresponding benzene core. It is noteworthy that the presence of carbohydrates with their tetraethylene glycol spacer properly counterbalanced the hydrophobic character of multiple benzene units surrounding each N₃P₃ center to furnish water-soluble compounds, even reaching a high

concentration (typically ~15 mg in 300 μL of D_2O). Notably, except for the small hexavalent **18**, similar solvodynamic diameters ranging from 5.3 to 7.2 nm were calculated, irrespective of the number of epitopes or branching units' sequences.

Table 2 Determination of diffusion data and solvodynamic diameters of multivalent conjugates by diffusion NMR spectroscopy experiments

Entry	Cpd	Valency	D ($\times 10^{-10} \text{ m}^2 \cdot \text{s}^{-1}$) ^a	d_s (nm)
<i>Acetylated dendrons</i> ^b				
1	15	5	3.10	2.6
2	29	15	1.57	5.1
3	31	25	1.19	6.8
<i>Acetylated macromolecules</i> ^b				
4	16	6	2.76	2.9
5	21	10	2.47	3.3
6	25	15	1.65	5.1
7	17	18	1.48	5.5
8	36	20	1.17	7.0
9	26	30	1.08	7.5
10	37	30	1.34	6.2
11	39	60	1.07	7.6
12	40	90	0.81	10.1
<i>Hydroxylated macromolecules</i> ^c				
13	18	6	1.10	3.6
14	22	10	0.75	5.3
15	27	15	0.70	5.7
16	19	18	0.67	5.9
17	28	30	0.56	7.2
18	38	30	0.65	6.2
19	41	90	0.60	6.6

^a See general procedures and the *Supporting Information* for extraction of the diffusion rate and calibration of the gradient strength. D was determined as the average value calculated from the decays of different proton resonances located at distinct levels in the structure.

^b Viscosity at 25°C for CDCl_3 : $\eta = 0.540 \text{ mPa}\cdot\text{s}$.

^c Viscosity at 25°C for D_2O : $\eta = 1.097 \text{ mPa}\cdot\text{s}$.

^d The error on the measurement was estimated for of the diffusion coefficients to be below 5%.

As reported by Fréchet *et al.*,⁴⁵ this observation might indicate that these pseudo-amphiphilic macromolecules have aromatic moieties tightly packed in the center and expose polar entities at the periphery. The linearity of the data related to these water-soluble dendrimers supported the absence of inter-molecular aggregation phenomena in solution, especially in more diluted conditions encountered in the following biochemical investigations (*See SI*). Obviously, bioactivity of the sugar headgroups is implied due to their presentation at the surface. In order to prove

this assumption, we performed an interaction study monitored by SPR.

SPR studies:

The relative binding affinities of several lactosylated dendrimers were evaluated by competitive SPR assays using two different galactoside-specific lectins: 1) a lectin from the Gram-negative bacterium *P. aeruginosa* (LecA)^{41,46} and 2) the proteolytically processed form of the human adhesion/growth-regulatory galectin-3 (trGal-3).⁴⁷ Both proteins have biomedical relevance. Homotetrameric LecA (or PA-IL) is a virulence factor that is involved in the pathogenesis of *P. aeruginosa* in immunocompromised or cystic fibrosis (CF) patients. Concerning Gal-3, this multifunctional protein has diverse physiological counter-receptors including glycan and peptide motifs, with roles in anoikis/apoptosis regulation, matrix interactions and autoimmune disease progression.⁴⁸ In its full-length form, *i.e.* with its tail of nine non-triple helical collagen repeats and a *N*-terminal peptide connected to the carbohydrate recognition domain, Gal-3 is able to readily form oligomers with polyvalent ligands.⁴⁹ Of note, proteolytic truncation by matrix metalloproteinases removes this *N*-terminal tail, with minor, if any, influence on glycan reactivity,^{47,49c} posing the question on its reactivity to multivalent glycans.

For the competitive inhibition studies, 3-[2-[aminoethyl]-thio]-propyl β -D-lactoside **42**⁵⁰ was immobilized onto the CM5 sensor surface (Biacore) by using the manufacturer's amide coupling methodology, to a level of ~230 RU (Figure 6). For the determination of IC_{50} values, equilibrium mixtures of lectins (1.5 μM for LecA and 7.5 μM for trGal-3) were incubated with increasing concentrations of glycodendrimers or monomeric references and used as analytes flowing over the surface of lactoside **42**. As a blank reference, ethanolamine was immobilized onto one path of the flow cell of the sensor chip (*See SI* for detailed protocols).

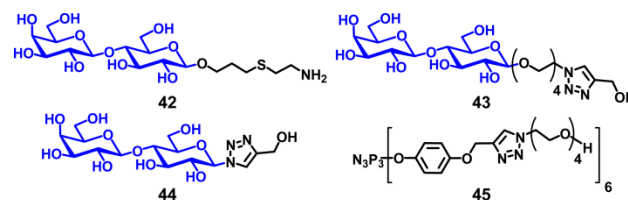


Figure 6. Structures of lactoside derivatives immobilized on the SPR chip (**42**), and monomeric references (**43** and **44**) for competitive SPR studies. CTP-based **45** represents a negative control.

To properly ascertain a cluster effect, monomeric reference

43 with the full linker was synthesized, together with its congener **44** without the tetraethylene glycol spacer. Furthermore, in order to exclude the influence of non-specific interactions generated by the dendritic template itself, a CTP core **45** containing 6 hydroxyl groups by the underivatized spacer was also used as a negative control

(See SI for syntheses of **43**, **44** and **45**). The affinity of both lectins towards the bound lactoside in the presence of different concentrations of glycodendrimers was measured and is reported in Table 3.

Table 3 IC₅₀ values of glycodendrimers and monomers derived from competitive inhibition SPR studies.

Cpd	Valency	LecA ^{a,b}			trGal-3 ^{a,b}		
		IC ₅₀ (μM)	r.p. ^c	r.p./sugar	IC ₅₀ (μM)	r.p. ^c	r.p./sugar
43	1	958 ± 34	1	1	164 ± 10	1	1
18	6	5.38 ± 0.14 ^d	178	30	0.55 ± 0.03	298	37
22	10	3.20 ± 0.20	299	30	0.31 ± 0.02	529	53
27	15	4.10 ± 0.20	233	16	0.39 ± 0.01	420	28
19	18	3.08 ± 0.30	311	17	0.38 ± 0.03	431	24
28	30	1.90 ± 0.18	504	17	0.30 ± 0.01	546	18
38	30	2.40 ± 0.11	399	13	0.22 ± 0.03	745	24
41	90	0.85 ± 0.09	1127	13	0.16 ± 0.01	1025	11

^a Non-specific interactions were not observable when negative control **45** was used. No signal observed for negative control αMe-Man.

^b The use of monomeric reference **44** as inhibitor generated IC₅₀ values above 2 mM for both lectins.

^c Relative potency.

^d The use of its congener containing 6 peripheral lactosides but lacking spacer moieties had an IC₅₀ of 30.8 μM with LecA.

In each case, simple exponential binding profiles were obtained (See SI for sensorgrams and related inhibitory curves). First, the IC₅₀ value for monomeric reference **43** and LecA is in the high micromolar range, which is consistent with the one previously published.^{11b} Overall, multivalent systems exhibited greatly improved affinity in both cases compared to reference **43**. More specifically, relative potencies for LecA approached 200 for the weakest ligand **18** with its six epitopes and exceeded 1000 for the best partner **41**. Although lactosides represent rather weak ligands for LecA,⁵¹ low millimolar values were obtained in our investigations for all the tested glycodendrimers, with an apparent “glycoside cluster effect” for the candidates **18** and **22** harboring six and ten epitopes, respectively. In these cases, a 30-fold potency enhancement of each lactoside located at the periphery was obtained in comparison to monomeric reference **43**. The benefit of the ethylene glycol repeats as aglycones was also investigated during comparative studies involving hexavalent **18** and its corresponding analog lacking the spacer, indicating a 6-fold decrease in activity for the latter. This observation may be attributed to both beneficial “aglycone-assisted” binding events⁵² and a favorable display of the epitopes. Interestingly, activities recorded for hexa-, deca-, pentadeca-, and octadecavalent systems (**18**, **22**, **27**, and **19**, respectively) compared very well with

that of the octadecavalent “onion peel” derivative described by our group in the same conditions.^{11b} Similar tendencies were observed with trGal-3: high nanomolar IC₅₀ values ranging from 550 to 160 nM were recorded. A gradual increase in activity was observed as a function of the scaffold valence increment for the entire series. In addition, a “dendritic effect” could be seen (r.p./sugar ≥ 11 in all cases). Using full-length Gal-3 and starburst glycodendrimers, their IC₅₀ values and corresponding relative inhibitory potencies had been determined from competitive solid-phase assays and indicated only a small enhancement of activity with increasing generation.⁵³ These observations were specific to Gal-3; significant increases in potency were observed for homodimeric Gal-1 and a plant toxin with two contact sites for sugars per subunit. Another observation concerned relative affinities per sugar (Table 3). The more potent multivalent constructs contained the lowest number of lactosides, notably for the dumbbell-shaped decavalent **22** (r.p./sugar = 53). Interestingly, this particular shape already proved more potent than globular cluster analogs in influenza virus-related investigations, so far without a clear explanation.⁵⁴ This tendency was seen for both lectins. Within the set of G(0) derivatives comprising **27**, **19**, **28**, and **38**, the variation of the central core was attributable to slight differences in affinity. Although both trivalent

conjugates **28** and **38** were constructed around distinct central cores but likely establishing a similar specific 2-fold tripodal orientation of the dendrons,^{32,37} different and divergent results were observed with the two lectins of separate design. Overall, all assays proved bioactivity of the sugar headgroups, encouraging systematic structure-activity studies, on a proof-of-principle basis.

In a nutshell, at this stage the results implied that a “dendritic effect” was more effective with low-valency derivatives, while overall activity linearly increased with ligands presenting a high density in epitopes. As consequence, relative potencies per sugar stagnated or diminished when more than 15 epitopes were at the periphery, and, as concluded from agglutination assays with vesicles,⁵⁵ not all the residues will likely participate in the mechanisms of action. Slight discrepancies also suggested that the scaffold itself may take an active part in the recognition process,⁵⁶ IC₅₀ values can reflect reassociation, the high density of ligands favoring consecutive rebinding, or sterical recognition process for high valency glycodendrimers. Interestingly, as recently highlighted by Widmalm *et al.*⁵⁷ with glycofullerenes, the accessibility of peripheral ligands represents a critical parameter for avidity, and the probability of interaction is enhanced when branching units with flexible linkers are used to locally increase ligand density. In our study, observed individual relative potencies for the conjugates may be biased by a lack of accessibility. In this respect, it is therefore intriguing that a surface display of lactosides with sub-maximal density in glycodendrimers obtained by self-assembly of amphiphilic Janus glycodendrimers gave optimal activity for galectin-dependent aggregation, this system providing an alternative vesicle (exosome/cell)-like platform for designing surface mimetics.^{36,58} Of note, the surface can be further tailored by implementing dendrimers, as membrane glycoproteins let branched *N*- and *O*-glycans become surface presented.¹³

Conclusions

This study describes synthetic aspects of dendrimer construction around phosphorous-based building blocks with tailored chemical modifications. The application of robust nucleophilic substitutions and Cu^I-catalyzed click chemistry, coupled with the use of hyper-functionalized and orthogonal branching units, resulted in multivalent architectures with a wide but tightly controlled structural diversity. In addition, the flexibility of this global approach allowed for the decoration of the constructs with saccharidic residues, providing tools to examine the

relation of topological sugar presentation to lectin activity, an example for an application of the synthetic products. The growth of sphere for functionalization was easily and straightforwardly achieved in a reduced number of synthetic steps and high-yielding chemical reactions. Hence, rapid generation of an elaborate family of multivalent conjugates comprising hypercores, hypermonomers, glycoclusters, dumbbell-shaped or globular glycodendrimers and heterogeneous “onion peel” analogs containing up to 90 lactose moieties as glycotopes, has been accomplished. Their integrity and desired uniformity were ascertained by classical multinuclear NMR spectroscopy and mass spectrometry together with additional biophysical diffusion NMR and GPC investigations. Competitive SPR studies performed with two different lectins taught us that 1) our synthetic approach furnished potent ligands with an enhancement in activity of each epitope presented at the periphery of the constructs as compared to a monomeric reference, even with non-optimized peripheral units and 2) the size, valency, shape and radial distribution of epitopes influenced the behavior of the derivatives as ligands. It appeared that the multiplication of CTP-layers was detrimental to the optimal presentation of terminal lactosides to the lectins in this case. Although glycodendrimers described herein appeared to adapt globular topologies as determined by diffusion NMR experiments, a recent study suggested that low generation cyclotriphosphazene-based structures with highly hydrophobic scaffolds and bearing terminal anionic azabisphosphonate groups may also access unidirectional conformations in response to biological receptors, this observed in molecular dynamics simulations in water.⁵⁹

Our initial results pave the way for further investigations towards the rationalization of the preferential binding mode(s). More specifically, considering the encouraging results for low-valency constructs, notably with dumbbell-shaped structures, complementary studies on symmetrical or Janus-type analogs built around AB₅, AB₁₅ or AB₂₅ wedge-like dendrons connected onto different spacers with adapted length and rigidity/flexibility balance could represent tempting additions to complete the series. On the side of the proteins, looking exemplarily at galectins, which of ten form a network *in situ*,⁶⁰ progress toward the design of inhibitors exploiting valency as discriminatory factor can be expected due to initial experience with triodobenzene/pentaerythriol-based glycoclusters and glycolaxarenes.^{49a,61} As ensuing perspective, considering the variety of synthetic approaches described in this work, CTP-scaffolds could represent useful dendritic templates

for the presentation of structurally optimized epitopes in anti-adhesins or in drug-targeting nanomaterials and as antigens in vaccination.²¹

Acknowledgments

‡ This work was supported by a discovery grant from the National Science and Engineering Research Council of Canada (NSERC) and by a Canadian Research Chair in Therapeutic Chemistry. Dr. X. Ottenwaelder (Concordia University, Montreal, Qc) is acknowledged for the X-ray crystallographic analysis of **1**. We are thankful to M.-C. Tang and Dr. A. Furtos (Université de Montréal, Montreal, Qc) for MALDI and ESI Mass spectrometry measurements and to V. Kriuchkov (Université du Québec à Montréal, Montreal, Qc) for GPC measurements.

Notes and references

^aPharmaqam, Department of Chemistry, University du Québec à Montréal, P.O. Box 8888, Succ. Centre-ville, Montréal, Québec, H3C 3P8, CANADA. Fax: +1-514-987-4054; Tel: +1-514-987-3000 ext 2546; E-mail: chabre.yoann@uqam.ca; roy.rene@uqam.ca

^bInstitute of Physiological Chemistry, Faculty of Veterinary Medicine, Ludwig-Maximilians-University, Veterinärstrasse 13, 80539 Munich, Germany

† Electronic Supplementary Information (ESI) available: Synthetic procedures and characterization, SPR studies, and crystallographic information (CIF file, CCDC deposition number 1415451). See DOI: 10.1039/b000000x/

- (a) F. Vögtle, G. Richardt and N. Werner, *Dendrimer Chemistry: Concepts, Syntheses, Properties, Applications*, Wiley-VCH, Weinheim, 2009; (b) S. Campagna, P. Ceroni and F. Puntoriero, *Designing Dendrimers*, John Wiley & Sons, Hoboken, New Jersey, 2012.
- (a) G. R. Newkome, C. N. Moorefield and F. Vögtle, *Dendrimers and Dendrons: Concepts, Synthesis, Applications*, Wiley-VCH, New York, 2001; (b) J. M. J. Fréchet and D. Tomalia, *Dendrimers and Other Dendritic Polymers*, John Wiley & Sons, New York, 2001; (c) T. Imae, in *Dendrimer-Based Drug Delivery Systems: From Theory to Practice*, Ed. Y. Cheng, John Wiley & Sons, New York, 2012, 55–92; (d) D. Astruc, E. Boisselier and C. Ornelas, *Chem. Rev.*, 2010, **110**, 1857–1959.
- (a) C. J. Hawker and J. M. J. Fréchet, *J. Am. Chem. Soc.*, 1990, **112**, 7638–7647; (b) C. J. Hawker, *Adv. Polym. Sci.*, 1999, **147**, 113–160.
- For seminal works: (a) E. Buhleier, W. Wehner and F. Vögtle, *Synthesis*, 1978, **2**, 155–158; (b) R. G. Denkwalter, J. Kolc and W. J. Lukasavage, *US Pat.*, 4,289,872, 1981; (c) D. A. Tomalia, H. Baker, J. Dewald, M. Hall, G. Kallos, S. Martin, J. Roeck, J. Ryder and P. Smith, *Polym. J.*, 1985, **17**, 117–132; (d) G. R. Newkome, Z. Yao, G. R. Baker and V. K. Gupta, *J. Org. Chem.*, 1985, **50**, 2003–2004.
- (a) M. Sowinska and Z. Urbanczyk-Lipkowska, *New J. Chem.*, 2014, **38**, 2168–2203; (b) M. V. Walter and M. Malkoch, *Chem. Soc. Rev.*, 2012, **41**, 4593–4609; (c) M. W. Walter and M. Malkoch, in *Synthesis of Polymers: New Structures and Methods*, Eds. A. D. Schlüter, C. J. Hawker, J. Sakamoto, Wiley-VCH

- Verlag GmbH & Co, 2012, 1027–1055; (d) X. Wang, Y. Yang, P. Gao, D. Li, F. Yang, H. Shen, H. Guo, F. Xu and D. Wu, *Chem. Commun.*, 2014, **50**, 6126–6129; (e) X.-X. Deng, F.-S. Du and Z.-C. Li, *ACS Macro Lett.*, 2014, **3**, 667–670; (f) J.-A. Jee, L. A. Spagnuolo and J. G. Rudick, *Org. Lett.*, 2012, **14**, 3292–3295; (g) A. Carlmark, C. Hawker, A. Hult and M. Malkoch, *Chem. Soc. Rev.*, 2009, **38**, 352–362; (h) V. Maraval, A.-M. Caminade, J.-P. Majoral and J.-C. Blais, *Angew. Chem.; Int. Ed. Engl.*, 2003, **42**, 1822–1826; (i) K. L. Wooley, C. J. Hawker and J. M. J. Fréchet, *Angew. Chem., Int. Ed. Engl.*, 1994, **33**, 82–85; (j) J. Camponovo, C. Hadad, J. Ruiz, E. Cloutet, S. Gatard, J. Muzart, S. Bouquillon and D. Astruc, *J. Org. Chem.*, 2009, **74**, 5071–5074; (k) K. L. Wooley, C. J. Hawker and J. M. J. Fréchet, *J. Am. Chem. Soc.*, 1991, **113**, 4252–4261.
- (a) F. Zeng and S. C. Zimmerman, *J. Am. Chem. Soc.*, 1996, **118**, 5326–5327; (b) C.-H. Wong and S. C. Zimmerman, *Chem. Commun.*, 2013, **49**, 1679–1695; (c) P. Antoni, D. Nyström, C. J. Hawker, A. Hult and M. Malkoch, *Chem. Commun.*, 2007, 2249–2251; (d) P. Antoni, M. J. Robb, L. Campos, M. Montanez, A. Hult, E. Malmström, M. Malkoch and C. J. Hawker, *Macromolecules*, 2010, **43**, 6625–6631; (e) J. W. Chan, C. E. Hoyle and A. B. Lowe, *J. Am. Chem. Soc.*, 2009, **131**, 5751–5753; (f) W. Wu, Z. Xu, W. Xiang and Z. Li, *Polym. Chem.*, 2014, **5**, 6667–6670.
- (a) M. B. Steffensen and E. E. Simanek, *Angew. Chem. Int. Ed.*, 2004, **43**, 5178–5180; (b) S. Patra, B. Kozura, A. Y.-T. Huang, A. E. Enciso, X. Sun, J.-T. Hsieh, C.-L. Kao, H.-T. Chen and E. E. Simanek, *Org. Lett.*, 2013, **15**, 3808–3811; (c) A. P. Goodwin, S. S. Lam and J. M. J. Fréchet, *J. Am. Chem. Soc.*, 2007, **129**, 6994–6995; (d) A. V. Ambade, Y. Chen and S. Thayumanavan, *New J. Chem.*, 2007, **31**, 1052–1063; (e) S. M. Grayson and J. M. J. Fréchet, *J. Am. Chem. Soc.*, 2000, **122**, 10335–10344.
- (a) S. Hecht, *J. Polym. Sci. Part A: Polym. Chem.*, 2003, **41**, 1047–1058; (b) K. Sivanandan, S. V. Aathimanikandan, C. G. Arges, C. J. Bardeen and S. Thayumanavan, *J. Am. Chem. Soc.*, 2005, **127**, 2020–2021; (c) M. Séverac, J. Leclaire, P. Sutra, A.-M. Caminade and J.-P. Majoral, *Tetrahedron Lett.*, 2004, **45**, 3019–3022; (d) T. Kang, R. J. Amir, A. Khan, K. Ohshimizu, J. N. Hunt, K. Sivanandan, M. I. Montañez, M. Malkoch, M. Ueda and C. J. Hawker, *Chem. Commun.*, 2010, **46**, 1556–1558; (e) M. E. Piotti, F. Rivera Jr., R. Bond, C. J. Hawker and J. M. J. Fréchet, *J. Am. Chem. Soc.*, 1999, **121**, 9471–9472; (f) C. Larre, D. Bressolles, C. Turrin, B. Donnadieu, A.-M. Caminade and J.-P. Majoral, *J. Am. Chem. Soc.*, 1998, **120**, 13070–13082.
- For example: (a) N. Katir, A. El Kadib, V. Collière, J.-P. Majoral and M. Bousmina, *Chem. Commun.*, 2014, **50**, 6981–6983; (b) C. Deraedt, N. Pinaud and D. Astruc, *J. Am. Chem. Soc.*, 2014, **136**, 12092–12098; (c) H.-F. Chow and J. Zhang, *Chem. Eur. J.*, 2005, **11**,

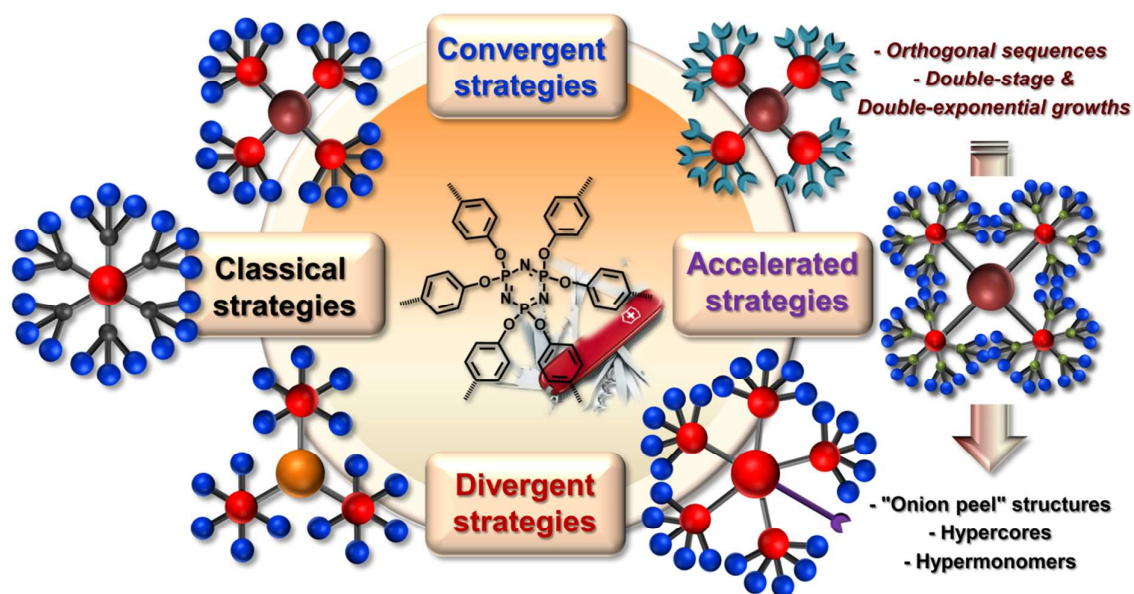
- 5817–5831; (d) M.-S. Choi, T. Aida, T. Yamazaki and I. Yamazaki, *Chem. Eur. J.* 2002, **8**, 12, 2667–2678.
- 10 (a) C. J. Hawker, K. L. Wooley and J. M. J. Fréchet, *Macromol. Symp.*, 1994, **77**, 11–20; (b) C. Hadad, J.-C. Garcia-Martinez and J. Rodriguez-Lopez, *J. Org. Chem.*, 2012, **77**, 6223–6230.
- 11 (a) R. Sharma, K. Naresh, Y. M. Chabre, R. Rej, N. Saadeh and R. Roy, *Polym. Chem.*, 2014, **5**, 4321–4331; (b) R. Sharma, N. Kottari, Y. M. Chabre, L. Abbassi, T. C. Shiao and R. Roy, *Chem. Commun.*, 2014, **50**, 13300–13003; (c) R. Sharma, I. Zhang, L. Abbassi, R. Rej, D. Maysinger and R. Roy, *Polym. Chem.*, 2015, **6**, 1436–1444; (d) N. Katir, N. El Brahmi, A. El Kadib, S. Mignani, A.-M. Caminade, M. Bousmina and J.-P. Majoral, *Chem. Eur. J.*, 2015, **21**, 6400–6408.
- 12 (a) R. M. Kannan, E. Nance, S. Kannan and D. A. Tomalia, *J. Int. Med.*, 2014, **276**, 579–617; (b) M. A. Mintzer and M. W. Grinstaff, *Chem. Soc. Rev.*, 2011, **40**, 173–190; (c) S. Svenson and D. A. Tomalia, *Adv. Drug Deliver. Rev.*, 2005, **57**, 2106–2129; (d) U. Boas and P. M. H. Heegaard, *Chem. Soc. Rev.*, 2004, **33**, 43–63; (e) M. W. Grinstaff, *Chem. Eur. J.*, 2002, **8**, 2838–2846; (f) U. Boas, J. B. Christensen and P. M. H. Heegaard, *Dendrimers in Medicine and Biotechnology—New Molecular Tools*, RSC Publishing, Cambridge, 2006.
- 13 (a) A. Varki, *Glycobiology*, 1993, **3**, 97–130; (b) C. Zuber, J. Roth in H.-J. Gabius, Ed. *The Sugar Code. Fundamentals of glycosciences*, Wiley-VCH, Weinheim, 2009, 87–110; (c) A. P. Corfield and M. Berry, *Trends Biochem. Sci.*, 2015, **40**, 351–359; (d) T. Henet and J. Cabalzar, *Trends Biochem. Sci.*, 2015, **40**, 377–384; (e) C. L. Schengrund, *Trends Biochem. Sci.*, 2015, **40**, 397–406; (f) R. W. Ledeen and G. Wu, *Trends Biochem. Sci.*, 2015, **40**, 407–418.
- 14 (a) H.-J. Gabius, Ed. *The Sugar Code. Fundamentals of glycosciences*, Wiley-VCH, Weinheim, 2009; (b) P. V. Murphy, S. André and H.-J. Gabius, *Molecules*, 2013, **18**, 4026–4053; (c) H.-J. Gabius, *Trends Biochem. Sci.*, 2015, **40**, 341; (d) H.-J. Gabius, H. Kaltner, J. Kopitz and S. André, *Trends Biochem. Sci.* 2015, **40**, 360–376; (e) D. Solís, N. V. Bovin, A. P. Davis, J. Jiménez-Barbero, A. Romero, R. Roy, K. Smetana Jr. and H.-J. Gabius, *Biochim. Biophys. Acta*, 2015, **1850**, 186–235.
- 15 J. Yariv, M. M. Rapport and L. Graf, *Biochem. J.*, 1962, **85**, 383–388.
- 16 (a) R. Kaufman and R. S. Sidhu, *J. Org. Chem.*, 1982, **47**, 4941–4947; (b) F. Perez-Balderas, J. Morales-Sanfrutos, F. Hernandez-Mateo, J. Isac-Garcia and F. Santoyo-Gonzalez, *Eur. J. Org. Chem.*, 2009, 2441–2453; (c) F. Perez-Balderas, M. Ortega-Munoz, J. Morales-Sanfrutos, F. Hernandez-Mateo, F. G. Calvo-Flores, J. A. Calvo-Asin, J. Isac-Garcia and F. Santoyo-Gonzalez, *Org. Lett.*, 2003, **5**, 1951–1954.
- 17 (a) Y. M. Chabre and R. Roy, *Adv. Carbohydr. Chem. Biochem.*, 2010, **63**, 165–393; (b) Y. M. Chabre and R. Roy, *Curr. Top. Med. Chem.*, 2008, **8**, 1237–1285; (c) R. Roy, *Trends Glycosci. Glycotechnol.*, 2003, **15**, 291–310; (d) N. Rockendorf and T. K. Lindhorst, *Top. Curr. Chem.*, 2001, **217**, 201–238; (e) W. B. Turnbull and J. F. Stoddart, *Rev. Molec. Biotechnol.*, 2002, **90**, 231–255; (f) R. Roy, D. Zanini, S. J. Meunier and A. Romanowska, *J. Chem. Soc., Chem. Commun.* 1993, 1869–1872.
- 18 (a) N. Sharon and H. Lis, *Essays Biochem.*, 1995, **30**, 59–75; (b) H. Rüdiger and H.-J. Gabius, *Glycoconjugate J.*, 2001, **18**, 589–613; (c) C. L. Nilsson, *Anal. Chem.*, 2003, **75**, 348A–353A; (d) H.-J. Gabius, S. André, J. Jiménez-Barbero, A. Romero and D. Solís, *Trends Biochem. Sci.*, 2011, **36**, 298–313; (e) S. André, H. Kaltner, J. C. Manning, P. V. Murphy and H.-J. Gabius, *Molecules*, 2015, **20**, 1788–1823.
- 19 (a) J. L. Lundquist and E. J. Toone, *Chem. Rev.*, 2002, **102**, 555–578; (b) N. Jayaraman, *Chem. Soc. Rev.*, 2009, **38**, 346–3483; (c) M. Mammen, S. K. Choi and G. M. Whitesides, *Angew. Chem. Int. Ed.*, 1998, **37**, 2754–2794; (d) R. Roy, *Curr. Opin. Struct. Biol.*, 1996, **6**, 692–702; (e) Y. C. Lee and R. T. Lee, *Acc. Chem. Res.*, 1995, **28**, 321–327.
- 20 (a) A. K. Michel, P. Nangia-Makker, A. Raz and M. J. Cloninger, *ChemBioChem*, 2014, **15**, 2106–2112; (b) S. André, S. Kojima, N. Yamazaki, C. Fink, H. Kaltner, K. Kayser and H.-J. Gabius, *J. Cancer Res. Clin. Oncol.*, 1999, **125**, 46–474; (c) H.-J. Gabius, *Cancer Invest.*, 1987, **5**, 39–46.
- 21 (a) T. C. Shiao and R. Roy, *New J. Chem.*, 2012, **36**, 324–339; (b) R. Roy and T. C. Shiao, *Chimia*, 2011, **65**, 24–29; (c) R. Roy, T. C. Shiao and K. Rittenhouse-Olson, *Braz. J. Pharm. Sci.*, 2013, **49**, 85–109.
- 22 (a) Y. M. Chabre and R. Roy, *Chem. Soc. Rev.*, 2013, **42**, 4657–4708; (b) Y. M. Chabre, A. Papadopoulos, A. A. Arnold and R. Roy, *Beilstein J. Org. Chem.*, 2014, **10**, 1524–1535; (c) N. V. Bovin and H.-J. Gabius, *Chem. Soc. Rev.*, 1995, **24**, 413–421; (c) For recent reviews: O. Renaudet and R. Roy, *Chem. Soc. Rev.*, 2013, **42**, 4515–4517 (Themed Issues “Multivalent Scaffolds in Glycoscience: An Overview”).
- 23 K. Rengan and R. Engel, *J. Chem. Soc., Perkin Trans. I*, 1991, 987–990.
- 24 As representative recent reviews: (a) A.-M. Caminade, A. Ouali, R. Laurent, C.-O. Turrin and J.-P. Majoral, *Chem. Soc. Rev.*, 2015, **44**, 3890–3899; (b) S. Mignani, S. El Kazzouli, M. M. Bousmina and J.-P. Majoral, *Chem. Rev.*, 2014, **114**, 1327–1342; (c) S. Mignani, S. El Kazzouli, M. M. Bousmina and J.-P. Majoral, *Adv. Drug Delivery Rev.*, 2013, **65**, 1316–1330; (d) O. Rolland, C.-O. Turrin, A.-M. Caminade, J.-P. Majoral, *New J. Chem.*, 2009, **33**, 1809–1824.
- 25 As vector for transfection: (a) C. Padié, M. Maszewska, K. Majchrzak, B. Nawrot, A.-M. Caminade and J.-P. Majoral, *New J. Chem.*, 2009, **33**, 318–326. As anti-HIV agents: (b) M. Blanzat, C. O. Turrin, A. M. Aubertin, C. Couturier-Vidal, A.-M. Caminade, J.-P. Majoral, I. Rico-Lattes and A. Lattes, *ChemBioChem*, 2005, **6**, 2207–2213. As drug carriers: (c) G. Spataro,

- F. Malecaze, C. O. Turrin, V. Soler, C. Duhayon, P. P. Elena, J.-P. Majoral and A.-M. Caminade, *Eur. J. Med. Chem.*, 2010, **45**, 326–334. As imaging agents: (d) O. Mongin, C. Rouxel, A. C. Robin, A. Pla-Quintana, T. R. Krishna, G. Recher, F. Tiaho, A.-M. Caminade, J.-P. Majoral and M. Blanchard-Desce, *Proc. SPIE-Int. Soc. Opt. Eng.*, 2008, **7040**, 704006.
- 26 H. R. Allcock and A. G. Scopelianos, *Macromolecules*, 1983, **16**, 715–719.
- 10 27 C. Hadad, J.-P. Majoral, J. Muzart, A.-M. Caminade and S. Bouquillon, *Tetrahedron Lett.*, 2009, **50**, 1902–1905.
- 28 (a) S. M. Rele, W. Cui, L. Wang, S. Hou, G. Barr-Zarse, D. Tatton, Y. Gnanou, J. D. Esko and E. L. Chaikof, *J. Am. Chem. Soc.*, 2005, **127**, 10132–10133; (b) E. Blattes, A. Vercellone, H. Eutamène, C.-O. Turrin, V. Théodorou, J.-P. Majoral, A.-M. Caminade, J. Prandi, J. Nigou and G. Puzo, *Proc. Natl. Acad. Sci. USA*, 2013, **110**, 8795–8800.
- 20 29 M. Touaibia and R. Roy, *J. Org. Chem.*, 2008, **73**, 9292–9302.
- 30 V. Maraval, R. Laurent, B. Donnadieu, M. Mauzac, A.-M. Caminade and J.-P. Majoral, *J. Am. Chem. Soc.*, 2000, **122**, 2499–2511.
- 25 31 E. Caverro, M. Zablocka, A.-M. Caminade and J. P. Majoral, *Eur. J. Org. Chem.*, 2010, 2759–2767.
- 32 (a) N. Lejeune, I. Dez, P.-A. Jaffrès, J.-F. Lohier, P.-J. Madec and J. Sopkova-de Oliveira Santos, *Eur. J. Inorg. Chem.*, 2008, 138–143; (b) E. Badetti, V. Lloveras, K. Wurst, R. M. Sebastián, A.-M. Caminade, J.-P. Majoral, J. Veciana and J. Vidal-Gancedo, *Org. Lett.*, 2013, **15**, 3490–3493.
- 30 33 (a) A.-M. Caminade, R. Laurent, C.-O. Turrin, C. Rebout, B. Delavaux-Nicot, A. Ouali, M. Zablocka and J.-P. Majoral, *C. R. Chimie*, 2010, **13**, 1006–1027; (b) A. Hameau, S. Fuchs, R. Laurent, J.-P. Majoral and A.-M. Caminade, *Beilstein J. Org. Chem.*, 2011, **7**, 1577–1583.
- 35 34 N. Jain, Y. Arntz, V. Goldschmidt, G. Duportail, Y. Mely and A. S. Klymchenko, *Bioconjugate Chem.*, 2010, **21**, 2110–2118.
- 40 35 M. Srinivasan, S. Sankararaman, H. Hopf, I. Dix and P. G. Jones, *J. Org. Chem.*, 2001, **66**, 4299–4303.
- 36 V. Percec, P. Leowanawat, H.-J. Sun, O. Kulikov, C. D. Nusbaum, T. M. Tran, A. Bertin, D. A. Wilson, M. Peterca, S. Zhang, N. P. Kamat, K. Vargo, D. Mook, E. D. Johnston, D. A. Hammer, D. J. Pochan, Y. Chen., Y. M. Chabre, T. C. Shiao, M. Bergeron-Brlek, S. André, R. Roy, H.-J. Gabius and P. A. Heiney, *J. Am. Chem. Soc.*, 2013, **135**, 9055–9077.
- 50 37 (a) G. R. Newkome and C. Shreiner, *Chem. Rev.*, 2010, **110**, 6338–6442; (b) Y. M. Chabre, C. Contino-Pépin, V. Placide, T. C. Shiao and R. Roy, *J. Org. Chem.*, 2008, **73**, 5602–5605.
- 55 38 (a) M. Meldal and C. W. Tornøe, *Chem. Rev.*, 2008, **108**, 2952–3015; (b) H. C. Kolb, M. G. Finn and K. B. Sharpless, *Angew. Chem. Int. Ed.*, 2001, **40**, 2004–2021; (c) P. Wu, A. K. Feldman, A. K. Nugent, C. J. Hawker, A. Scheel, B. Voit, J. Pyun, J. M. J. Fréchet, K. B. Sharpless and V. V. Fokin, *Angew. Chem. Int. Ed.*, 2004, **43**, 3928–3932; (d) B. T. Worrell, J. A. Malik and V. V. Fokin, *Science*, 2013, **340**, 457–460; (e) S. Dedola, S. A. Nepogodiev and R. A. Field, *Org. Biomol. Chem.*, 2007, **5**, 1006–1017; (f) V. Aragão-Leoneti, V. L. Campo, A. S. Gomes, R. A. Field and I. Carvalho, *Tetrahedron*, 2010, **66**, 9475–9492; (g) B. Schulze, and U. S. Schubert, *Chem. Soc. Rev.*, 2014, **43**, 2522–2571.
- 60 39 X. Sheng, T. C. Mauldin and M. R. Kessler, *J. Polym. Sci.: Part A: Polym. Chem.*, 2010, **48**, 4093–4102.
- 70 40 N. Kottari, Y. M. Chabre, T. C. Shiao, R. Rej and R. Roy, *Chem. Commun.*, 2014, **50**, 1983–1985.
- 41 Y. M. Chabre, D. Giguère, B. Blanchard, J. Rodrigue, S. Rocheleau, M. Neault, S. Rauthu, A. Papadopoulos, A. A. Arnold, A. Imberty and R. Roy, *Chem. Eur. J.*, 2011, **17**, 6545–6562.
- 75 42 Y. Cohen, L. Avram and L. Frish, *Angew. Chem. Int. Ed.*, 2005, **44**, 520–554.
- 43 D. Wu, A. Chen and C. S. Johnson Jr., *J. Magn. Reson. Series A*, 1995, **115**, 260–264.
- 80 44 S. Berger, and S. Braun, *200 and More NMR Experiments—A Practical Course*, Wiley-VCH, Weinheim, 2004, 145–148.
- 45 I. Gitsov and J. M. J. Fréchet, *J. Am. Chem. Soc.*, 1996, **118**, 3785–3786.
- 85 46 (a) D. Avichezer, D. J. Katcoff, N. C. Garber and N. Gilboa-Garber, *J. Biol. Chem.*, 1992, **267**, 23023–23027; (b) G. Cioci, E. P. Mitchell, C. Gautier, M. Wimmerova, D. Sudakevitz, S. Pérez, N. Gilboa-Garber, A. Imberty, *FEBS Lett.*, 2003, **555**, 297–301; (c) C. P. Chen, S. C. Song, N. Gilboa-Garber, K. S. Chang, A. M. Wu, *Glycobiology*, 1998, **8**, 7–16.
- 90 47 J. Kopitz, S. Vértésy, S. André, S. Fiedler, M. Schnölzer and H.-J. Gabius, *Biochimie*, 2014, **104**, 90–99.
- 95 48 (a) S. Akahani, H. Inohara, P. Nangia-Makker and A. Raz, *Trends Glycosci. Glycotechnol.*, 1997, **9**, 69–75; (b) H. Sanchez-Ruderisch, C. Fischer, K. M. Detjen, M. Welzel, A. Wimmel, J. C. Manning, S. André and H.-J. Gabius, *FEBS J.*, 2010, **277**, 3552–3563; (c) H. Kaltner and H.-J. Gabius, *Histol. Histopathol.*, 2012, **27**, 397–416; (d) H. Dawson, S. André, E. Karamitopoulou, I. Zlobec and H.-J. Gabius, *Anticancer Res.*, 2013, **33**, 3053–3059; (e) S. Toegel, D. Bieder, S. André, K. Kayser, S. M. Walzer, G. Hobusch, R. Windhager and H.-J. Gabius, *Histochem. Cell Biol.*, 2014, **142**, 373–388.
- 100 49 (a) S. André, B. Liu, H.-J. Gabius and R. Roy, *Org. Biomol. Chem.*, 2003, **1**, 3909–3916; (b) N. Ahmad, H.-J. Gabius, S. André, H. Kaltner, S. Sabesan, R. Roy, B. Liu, F. Macaluso and C. F. Brewer, *J. Biol. Chem.*, 2004, **279**, 10841–10847; (c) T. K. Dam, H.-J. Gabius, S. André, H. Kaltner, M. Lensch and C. F. Brewer, *Biochemistry*, 2005, **44**, 12564–12571.
- 110

- 50 M. P. Dubois, C. Gondran, O. Renaudet, P. Dumy, H. Driguez, S. Fort and S. Cosnier, *Chem. Commun.*, 2005, 4318–4320.
- 51 (a) J. Rodrigue, G. Ganne, B. Blanchard, C. Saucier, D. Giguère, T. C. Shiao, A. Varrot, A. Imberty and R. Roy, *Org. Biomol. Chem.*, 2013, **11**, 6906–6918; (b) A. Imberty, Y. M. Chabre and R. Roy, *Chem. Eur. J.*, 2008, **14**, 7490–7499; (c) J.-L. Reymond, M. Bergmann and T. Darbre, *Chem. Soc. Rev.*, 2013, **42**, 4814–4822.
- 52 (a) N. Sharon, *FEBS Lett.*, 1987, **217**, 145–157; (b) P. Arya, K. M. K. Kutterer, H. Qin, R. Huiping, J. Roby, M. L. Barnes, J. M. Kim and R. Roy, *Bioorg. Med. Chem. Lett.*, 1998, **8**, 1127–1132.
- 53 S. André, P. J. C. Ortega, M. A. Perez, R. Roy and H.-J. Gabius, *Glycobiology*, 1999, **9**, 1253–1261.
- 54 (a) K. Hatano, K. Matsuoka and D. Terunuma, *Chem. Soc. Rev.*, 2013, **42**, 4574–4598; (b) K. Hatano, T. Matsubara, Y. Muramatsu, M. Ezure, T. Koyama, K. Matsuoka, R. Kuriyama, H. Kori and T. Sato, *J. Med. Chem.*, 2014, **57**, 8332–8339; (c) H. Oka, T. Onaga, T. Koyama, C.-T. Guo, Y. Suzuki, Y. Esumi, K. Hatano, D. Terunuma and K. Matsuoka, *Bioorg. Med. Chem.*, 2009, **17**, 5465–5475.
- 55 C. M. W. Grant, M. W. Peters, *Biochim. Biophys. Acta* 1984, **779**, 403–422.
- 56 M. L. Talaga, N. Fan, A. L. Fueri, R. K. Brown, Y. M. Chabre, P. Bandyopadhyay, R. Roy and T. K. Dam, *Biochemistry*, 2014, **53**, 4445–4454.
- 57 O. Engström, A. Muñoz, B. M. Illescas, N. Martin, R. Ribeiro-Viana, J. Rojo and G. Widmalm, *Org. Biomol. Chem.*, 2015, **13**, 8750–8755.
- 58 (a) S. Zhang, R.-O. Moussodia, H.-J. Sun, P. Leowanawat, A. Muncan, C. D. Nusbaum, K. M. Chelling, P. A. Heiney, M. L. Klein, S. André, R. Roy, H.-J. Gabius and V. Percec, *Angew. Chem. Int. Ed.*, 2014, **53**, 10899–10903; (b) S. Zhang, R.-O. Moussodia, C. Murzeau, H. J. Sun, M. L. Klein, S. Vértesy, S. André, R. Roy, H.-J. Gabius and V. Percec, *Angew. Chem. Int. Ed.*, 2015, **54**, 4036–4040; (c) S. Zhang, R.-O. Moussodia, S. Vértesy, S. André, M. L. Klein, H.-J. Gabius and V. Percec, *Proc. Natl. Acad. Sci. USA*, 2015, **112**, 5585–5590.
- 59 A.-M. Caminade, S. Fruchon, C.-O. Turrin, M. Poupot, A. Ouali, A. Maraval, M. Garzoni, M. Maly, V. Furer, V. Kovalenko, J.-P. Majoral, G. M. Pavan and R. Poupot, *Nat. Commun.*, 2015, DOI: 10.1038/ncomms8722.
- 60 (a) H. Kaltner, D. Kübler, L. López-Merino, M. Lohr, J. C. Manning, M. Lensch, J. Seidler, W. D. Lehmann, S. André, D. Solís, H.-J. Gabius, *Anat. Rec.*, 2011, **294**, 427–444; (b) E.-M. Katzenmaier, S. André, J. Kopitz, H.-J. Gabius, *Anticancer Res.*, 2014, **34**, 5429–5438.
- 61 (a) S. André, F. Sansone, H. Kaltner, A. Casnati, J. Kopitz, H.-J. Gabius, R. Ungaro, *ChemBioChem.*, 2008, **9**, 1649–1661; (b) S. André, C. Grandjean, F. M. Gautier, S. Bernardi, F. Sansone, H.-J. Gabius, R. Ungaro, *Chem. Commun.*, 2011, **47**, 6126–6128.

60

Table of contents (TOC)



Cyclotriphosphazene-based building-blocks were successfully used as versatile synthetic multi-tools for the efficient and straightforward construction of multifaceted bioactive glycoclusters and glycodendrimers. This synthetic approach furnished potent ligands for a bacterial virulence factor (LecA) and a human adhesion/growth-regulatory lectin (trGal-3).